Mechanism of Catalytic Behavior and Structure

of Active Centers in CuY Zeolite

Shuji Tanabe and Hiroshige Matsumoto

Abstract

The experimental and theoretical basis for the activated coppere xchanged Y zeolite system have been studied by the observation and analysis in the electronspin resonanace (ESR), infrared (IR) and extended X-ray absorption fine structure (EXAFS) spectroscopies.

Introduction

Zeolites are crystalline aluminosilicates with a chemical composition $M^{n+}_{x/n}[(AlO_2^-)_x(SiO_2)_y]_z H_2O$ where M^{n+} is the cations which balance the negative charge associated with the framework aluminum ions. The framework atoms of Si and Al, are each tetrahedrally coordinated to four oxygen atoms. The periodic three-dimensional network, which is characteristic of zeolites, is formed by linking the (SiO_4) and (AlO_4) tetrahedra through shared oxygen ions. These tetrahedra tend to form rings, containing from four to twelve units of the tetrahedra.
Such rings normally form the entrances to channels or cages in zeolites and thus define the pore diameter for a particular structure.

Synthetic zeolite A, X, and Y all consist of tetrahedra linked to form truncated-octahedra or so-called sodalite cage units. When these units are linked through four-membered rings zeolite A is formed, whereas linking via the six-membered rings in zeolite X and Y. The latter two zeolite only differ in the Si /Al ratio. In general, zeolites, especially Y zeolite, have good thermal stability, but this is further improved by increasing in the Si/Al ratio. The hydrothermal stability of zeolites also increases with decreasing aluminum content.

The charge-compensating cations in the synthetic zelites, originally sodium ions, can be exchanged for other cations of different type and/or valency. However, great cares must be taken during ion exchange to avoid

strongly acidic solutions which can lead to proton exchange with the zeolite metal cations or even structure collapse. The more silica-rich zeolites such as mordenite and ZSM-5, however, are stable under such conditions.

Acid sites can be introduced into zeolites in a number of different ways: (1) ion exchange with NH_4^+, followed by thermal decomposition, i. e., NH_4^+ $Z^- \to H^+Z^- + NH_3(g)$, (2) hydrolysis of ion-exchanged polyvalent cations follow-ed by partial dehydration, i. e., $M(H_2O)_x{}^{n+}Z^- \to M(OH)^{(n-1)+}Z^- + H^+Z^- +$ (X-1)H_2O, (3) direct proton exchange, i.e., $Na^+Z^- + H^+ \to H^+Z^- + Na^+$, (4) reduction of exchanged metal ions to a lower valency state, i.e., $Mn^+Z^- + 1/2 H_2 \to$ $M^{(n-1)+}Z^- + H^+Z^-$. The so-formed proton or Bronsted acid sites can be further dehydroxylated to form tricoordinated aluminum sites, Lewis acid sites, i.e.,
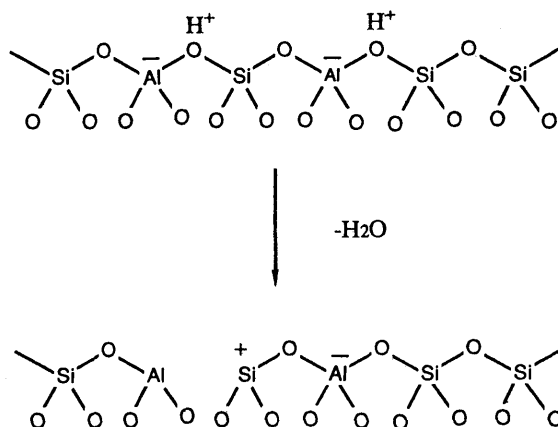
The location of cations in zeolite lattice are complicated because of the large numbers of potential sites. In general, most of the cations lie along the crystallographic three fold axes of the cubic unit cell. Various positions along these axes have been arbitrarily given Roman numbers, as shown in Fig. 1. Only the site II cations on these axes, whichi are located at the six-membered rings, are able to interact with adsorbate molecules present in the supercages. Access to the smaller sodalite cages is severely limited by the small diameter (2. 2 Å) of the six-ring entrance. Thus, only small ligands such as NH_3 and H_2O may enter the small cavities (sodalite cages). Addi-tional sites (so-called as Sites-III) has been identified in the supercage, near the four-membered rings which link adjacent sodalite cages. There is good evidence that ions located at these sites are the active entities for hexane de-hydrocyclization over TeNaX[1] and butadiene cyclodimerization over CuNaY.[2]
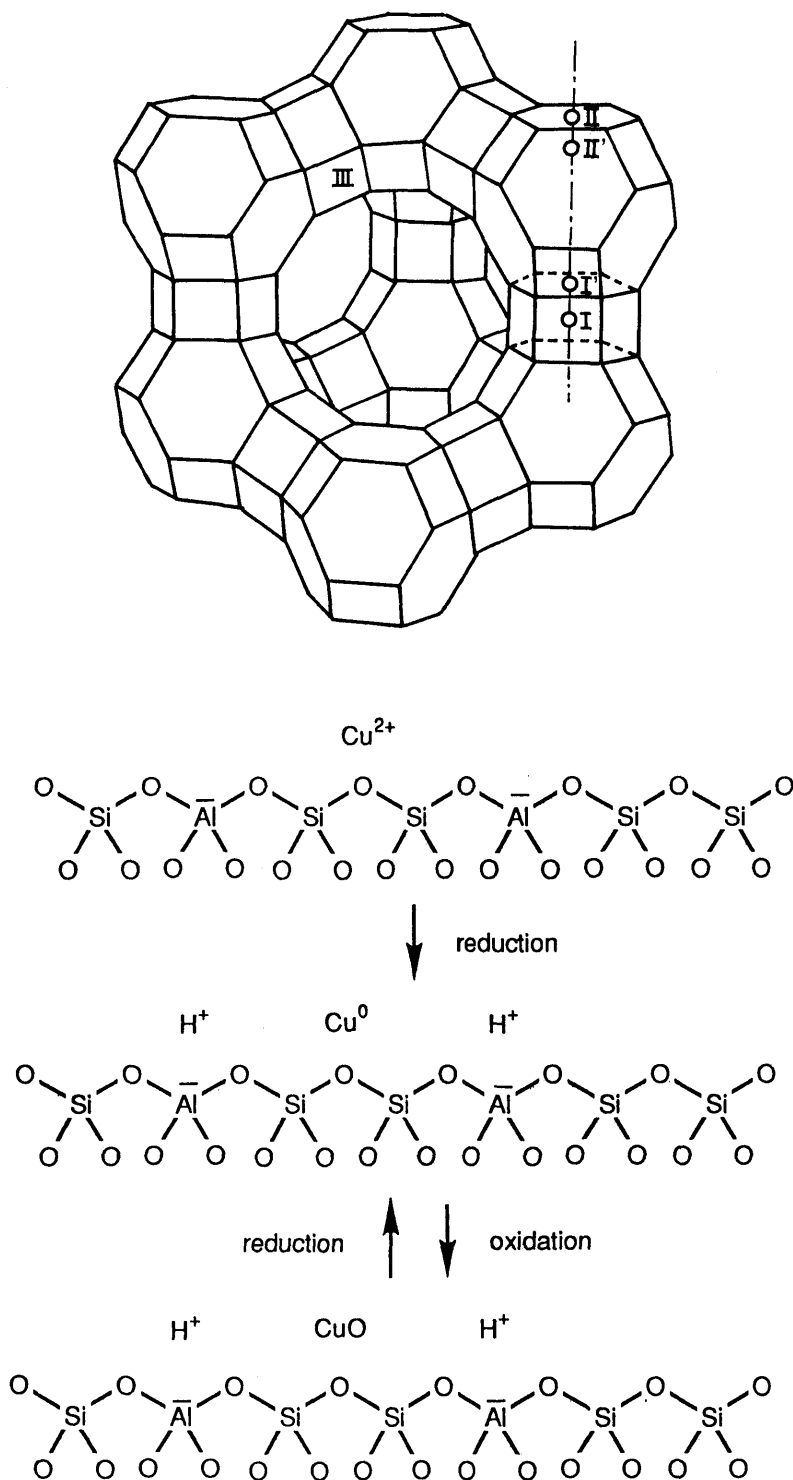
Fig. 1   Stereodiagram of the faujasite-framework and cation siting.

The location of site III at the entrance to the supercages, together with the unsaturated coordination geometry of the cations, provides an ideal site for interaction with adsorbate molecules.

Although these cations occupy specific sites of the zeolite, they are continuously hopping from one site to another on the time scale of minutes at room temperature. This means that particular ions which might be in an inuccessible site (e.g. site I) at one moment would be available for coordination with a ligand in the large cavity at some late time. All of the cations become available to form coordination complexes in the large cavities and will do so provided the energetics for coordination are favorable.

The site occupancy and nature of charge compensationin zeolites are related to the problem of charge distribution in the framework. The occupancy of several sites in zeolite by various cations is given in a compendium by Mortier.[3] In a dehydrated CuY zeolite which contains, for example, 16 Cu^{2+} ions per unit cell there are 3.2 ions in site I, 11.1 ions in site I' and 1.7 ions which cannot be characterized by X-ray diffraction.[4]

During the last three decades there have been considerable academic and industrial researches carried out in the field of zeolite catalysis. The greater part of these works has, however, been related to reactions where the synthetic zeolite is used as solid acid catalysts, e.g., the zeolites are excellent catalysts in isomerizations, crackings, decompositions and polymerizations. This is hardly surprising since this area represents the major application to date of zeolites as catalysts in industrial process. Reviews on zeolite catalysis have therefore also in general tended to concentrate more on the work related to acid catalysis.[5-7] In principle, synthetic zeloites offer considerable scope for surface modification. The ion-exchange properties and the periodicity of zeolite frameworks are, for example, enable functional metal ions or complexes to be stabilized in a bariety of oxidation states and coordination geometries on specific surfaces in a well-defined pore structure. This represents a valuable starting point in the design of catalytic surfaces.

On the other hand, zeolites with transition metal ionshave been successfully applied to reactions such as oxidation, reduction, olefin oligomerization, carbonylation, hydroformylation, synthesis gas conversion, and water splitting. A greater emphasis is given to the most recent and more novel applications of zeolites to heterogeneous catalysis.

The oxidation of CO is widely used as a test reaction for oxidation catalysts because of its simplicity. Thus, there is quite an extensive literature on CO oxidation using various catalysts. The parent zeolite of Na forms show

very little oxidation activity and therefore the majority of the studies have concentrated on ion-exchanged forms with transition metals.

It is of particular interest to compare the relative activities of these ion-exchanged zeolites with the corresponding oxides in order to gain some insight into the influence of the zeolite lattice. Boreskov et al.[8] compared the specific activities of CuY and CuO in CO oxidation calculated on the basis of surface copper concentrations. Although the specific activity of CuY increases with increasing copper content, even at 16 wt % Cu the activity is 2.5 orders of magnitude less than that of CuO. Beyer et al. carried out a detailed kinetic study on CO oxidation over CuNaY zeolite after various pretreatments. The results obtained were explained in terms of the ralative concentrations of the species Cu^{2+}, Cu^+, and Cu^0 present in each catalysts.[9] Williamson et al. showed that Cu^{2+} Y was an active catalyst for the oxidation of NH_3 to N_2 and H_2O. A mechanism was proposed involving the intermediate formation of an amine complex $[Cu(NH_3)_4]^{2+}$. The NH_3 reduction of Cu^{2+} to Cu^+ in this complex was proposed as the slow step with reoxidation via O_3 being very rapid. This mechanism was consistent with the kinetic expressions which were shown to be first order in NH_3 and zero order in O_2. A similar behavior has also been demonstrated 10, 11 for Fe, Ni, Co, and Cr ions exchanged into Y zeolite and compared with corresponding oxides (i.e., α-Fe_2O_3, NiO, Co_3O_4, and Cr_2O_3). In addition, the activation energies for the transition metal ion-exchanged zeolites are considerably higher than those for the corresponding oxides (e.g., CuY, 19.5 kcal/mol; CuO, 13 kcal/mol; NiY, 26 kcal/mol; NiO, 9.5 kcal/mol). For transition metal ion-exchanged zeolites X and Y, the activities for CO oxidation increase exponentially with increasing metal ion standard oxidation potential (i.e., $Cu^+ > Fe^{2+} > Cr^{3+} > Cu^{2+} = Ni^{2+}$).[12]

It has been shown[13-16] also that the equilibrated pH of the transition metal ion-exchange solution is also critical in determining the specific activity of zeolitecatalysts. The influence of both transition metal ion loading and pH of ion-exchange solution has been attributed to the formation of active metal oxygen bridge species within the zeolite cavities (i.e., M^{n+}-O_2-M^{n+}) where the anions corresponding are considered to be extralattice (i.e., non-zeolite framework) oxide ions. The formation of such species would be expected to be favored by high metal loadings and hydrolysis conditions during ion exchange, as is observed. In fact there are some direct evidences from ESR[16], Mossbauer spectroscopy,[17] IR spectroscopy[18], and magnetic measurements[15] to support the existence of these oxygen-bridged species.

The oxidative dehydrogenation of cyclohexane to benzene has been

studied more extensively. Transition metal ion-exchanged forms of zeolite Y have been shown to be particularly active catalysts for this reaction.[19-21] Although the platinum metal ions exhibit the highest activity, CuY was found to be the most selective for benzene formation.[20, 21]

The catalytic behavior of the Cu-exchanged zeolite markedly depends on the treatment prior to catalysis. With respect to CuY zeolite as the catalyst in oxidation reaction, one of the most important factors is the oxidation state of Cu component, which governs the quality and quantity of the catalytic centers. It can be roughly considered as shown the following scheme that uponreduction of Cu^{2+} ions balanced with the negative charges of AlO_4 tetrahedra transform into Cu metal, which is reoxidized into CuO particles or back to the original Cu^{2+} ions.

Cu^{2+}

[Structural scheme of Si–O–Al–O–Si zeolite framework]

Oxidation ↑ ↓ Reduction

H^+ Cu^0 H^+

[Structural scheme of Si–O–Al–O–Si zeolite framework]

Reduction ↑ ↓ Oxidation

H^+ CuO H^+

[Structural scheme of Si–O–Al–O–Si zeolite framework]
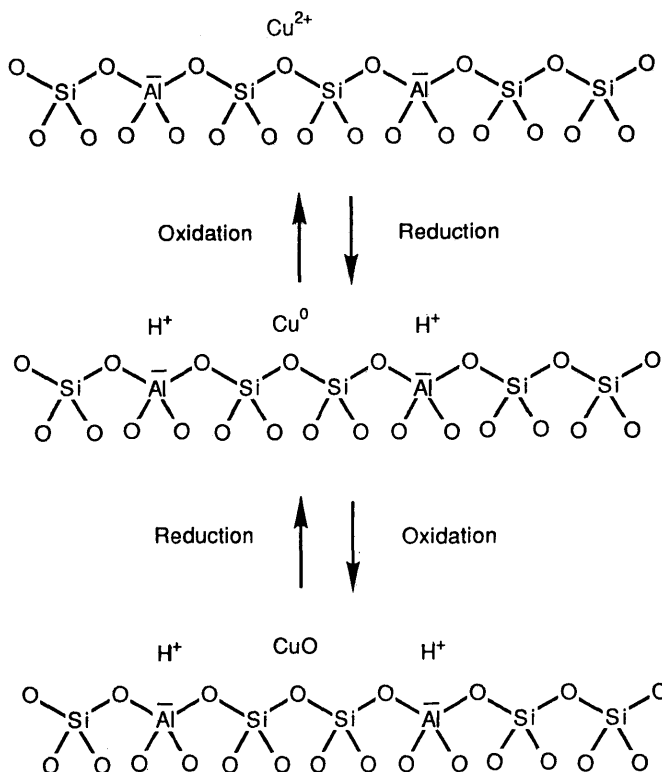
Objectives of this study are investigations in the process of formation and characterization of the catalytically active species in CuY zeolite. It the first-objective, the formation of an active species has been recognized by a consecutive reduction-reoxidation (R-O) treatment of CuY sample under very mild conditions. The R-O treatment consists of three stages, i.e., the dehydration process by evacuation, reduction process with hydrogen and reoxida-

tion process with oxygen.   The catalytic activity of CuY zeolite are closely related to the oxidation state of Cu species in the matrix, which has been investigated using various physico-chemical techniques, as described before. Among these techniques the temperature-programmed reduction (TPR) is considered to be one of the simplest methods in the studies of oxidation state of Cu species.   In this study, from this point of view, the formation of the active species in CuY zeolite by an activation has been investigated by the TPR technique and the amount of this species has been related to their catalytic activity in a CO oxidation at low temperatures.   .

In the second objective, the structural changes of Cu species in the zeolite matrix have been followed by the measurements of K-edge extended X-ray absorption fine structure (EXAFS) spectroscopy.   That is, the characteriza- tion of CuY zeolite activated by a consecutive reduction-reoxidation (R-O) treatment had been made by the EXAFS measurements in the sequence of each step during the course of TPR process and catalysis.   The particle sizes of Cu species formed in CuY with the R-O treatment are so small that conventional techniques, such as X-ray diffraction spectroscopy (XRD) and transmission electronmicroscopy, are incompetent to investigate them.   The EXAFS spectroscopy is well suited for this purpose since it can pursue changes of local structure around Cu atoms.   The present work has summarized the researches already reported in the references a-h.

Experimental

Preparation of CuY catalyst

Linde LZY−52 NaY zeolite, Lot No.3606468, $Na_{50}(AlO_2)_{50}(SiO_2)_{118}$, was used as the starting material.   The zeolite was ion-exchanged in a 0.1 mole dm^{-3} solution of $(CH_3COO)_2$ Cu with the zeolite/solution ratio of 50g/1000 cm^3.   The exchange was conducted overnight at room temperature and repeated three times.   The sample was washed with distiled water until no cupric ions was detected in the filtrate, and dried overnight at 383 K in an oven.   The dried sample was pelletized, crushed into particles from 16 to 32 mesh, and stored over a saturated ammonium chloride solution to control the adsorbed water constant.   The amount of copper(II) ions in the zeolite was determined by atomic absorption measurement.   In this procedure 59.6% of Na^+ ions were replaced by Cu^{2+} ions without substantial loss of crystal- linity.   The chemical composition of the sample obtained, therefore, is

roughly expressed by $Cu_{15} Na_{20} (AlO_2)_{50}(SiO_2)_{118}$.

Activation of CuY zeolite

The activation of CuY zeolite by a consecutive reduction and reoxidation (R-O) treatment was performed under mild conditions in a conventional circulation system, as shown in Fig. 2. Basically, the apparatus consists of a

Vaccum Pump

M.F.C.   P.T.   C.P.   GC

He   H2   O2   CO

Trap

Sample
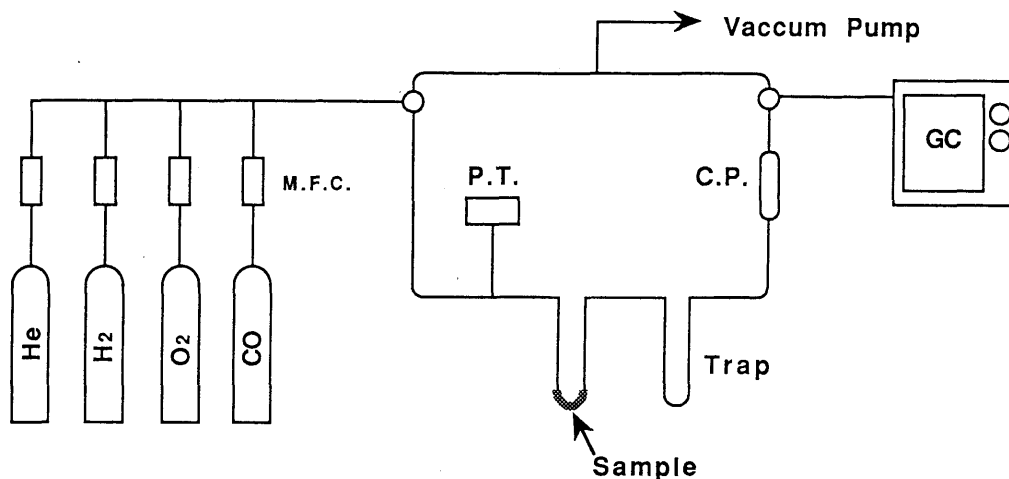
Fig. 2 Schematic diagram of the flow/circulation system.

quartz U-type reactor, a high speed circulation pump, liquid nitrogen trap, and a pressure transducer (MKS 222-B) connected with a microcomputer (NEC PC-9801). The R-O treatment consists of three consecutive stages, preliminary evacuation, reduction with hydrogen, and reoxidation with oxygen. In the first stage the sample was evacuated at room temperature for 0.5 h and the at desired temperature for 0.5 h. This series of evacuation was carried out for all samples tested in order to control the amount of water adsorbed on the surface. Reduction of the evacuated sample was carried out with hydrogen at desired temperature for 2 h under the initial pressure of 10 kPa. The reduced sample was the reoxidized with oxygen at ambient temperatures also for 2 h under 10 kPa.

Measurements of temperature-programmed reduction

The TPR measurements were performed in the same circulation system used in the activation process. The hydrogen consumption during the TPR

process was estimated from pressure decrease in the system. The pressure changecorresponding to 1 μmol could be detected by this apparatus. The data were recorded in the microcomputer for calculation. The volume of hydrogen consumed was calculated by $C = \Delta p\, V / (22400\, W)$ where C is the hydrogen consumption (mol g^{-1}), Δp is pressure decrease (torr), V is the volume of circulation system (231.4 cm^3), and W is the weight of sample in dry base (g). In the TPR measurement, an extra pure hydrogen was introduced onto a small aliquot (0.6 g in dry base) ofthe sample under the initial pressure of 10.0 kPa and temperature of the reactor was linearly raise at a rate of 5 K min.$^{-1}$

Measurements of electron spin resonance spectra

In order to examine the oxidation state of Cu^{2+} ions in zeolite during the R-O treatment, measurements of electron spin resonance (ESR) were carried out using a JEOL (JES PE-1 X) spectrometer. The instrument was operated in the X-band region at 9.3 GHz. The g values were determined by comparison with that of Mn^{2+} ions (g$_1$ =1.981) on magnesium oxide. The standard sample was attached to the outside on the sample tube containing 300mg of the granular CuY zeolite. The ESR spectra were recorded at room temperature.

Measurements of infrared spectra

The formation of Cu$^+$ ions was checked by an IR spectroscopy. The IR measurements were carried out with JASCO (A-100) spectrometer. The zeolite powder of 10 mg was pressed into thin wafers between stainless steel plates under a pressure of 10 tons. The sample wafer was placed in the center of the in situ cell with KBr windows and a heating coils. The IR spectra were recorded at room temperature after each treatment.

Measurements of catalytic activity

The catalytic activity of CuY zeolite was measured in the CO oxidation with oxygen at low temperatures between 373 and 433 K under atmospheric pressure. The kinetic measurement was carried out by the flow system in a differential reactor with small amount of catalyst and high velocity of gas flow. The system basically consists of a gas-feeding manifold with mass-

flow controllers, a quartz reactor, sampling valves, and a gas chromatography for analysis. The gas chromatograph used was Shimazu GC- 8 AIT with active carbon column (30-60 mesh), operated at 333 K in an oven. The react or is connected to the circulation system in order to perform the R-O treatm ent in the exactly same condition to that in the case of TPR experiment. The reactant gas used in the catalysis was the mixture of 2.5 % CO_2 and 10 % O_2 in helium.

Measurements of extended X-ray absorption fine structure spectra

The EXAFS measurements were performed by an "in situ" system which has been described in detail elsewhere. Basically it consists of a rotating anode X-ray generator (Rigaku RU-200), a spectrometer with a bent sillicon (220) crystal by Johansson cut, ion chambers, slits and counting eledtronics by a computer through CAMAC bus. The X-ray source with a silver target was operated at 14 kV and 200 mA to minimize the effect of higher order re- flections on the ion chamber. The CuY samples were pressed into thin wafers and treated in the similar ways to the measurements in TPR, R-O treatment and activity test. In the preparation of samples for EXAFS measurements, 300 mg of CuY sample was pressed into thin wafer. The wafer was mounted in the center of in situ cell made of Pyrex grass with beryllium windows. Prior to measurements of the EXAFS spectra, the CuY samples were treated in the similar ways to the TPR and R-O treatment.

Analysis of EXAFS data

Detailed method in data analysis has also beendescribed elsewhere. A single scattering model for EXAFS oscillations is expressed by

$$\chi(k) = \sum_j \frac{Nj}{kR_j^2} \exp[-2(\sigma_j^2 k^2 + R_j/\lambda)] F_j(\pi, k) \sin(2kR_j + \alpha_j(k)) \quad (1)$$

where k is the photoelectron wave vector, N_j is the number of atoms in the jth shell, R_j is the distance from the central Cu atoms, F_j is the scattering ampli- tude, σ_j is Debye-Waller factor, and α_j is the phase shift. The meanfree path of the photoelectron in the solid, λ, is assumed to be independent of k in this work. The EXAFS functionis Fourier transformed by weighting k^3 to yield the radial distribution function, $\Phi(R)$, as follows:

$$\Phi(R) = \sqrt{\frac{1}{2}} \int k^3 \chi(k) \exp(-2\pi kR) dk \qquad\qquad (2)$$

The curve-fitting procedures are employed to determine structural parameters, such as R and N.   The main peaks in the radial distribution function are inverse-transformed into k space and a least-squares calculations are made by using equation (1).

Results and Discussion

TPR profile of CuY with R-O treatment

It has already been known that the reduction of Cu^{2+} ions in the original form of CuY zeolite with hydrogen occurs by two-step mechanism, via Cu^+ ions to Cu metal.   A profile of the two-step reduction could be demonstrated clearly by TPR spectra obtained under appropriate conditions, such as a low temperature in the preliminary evacuation, a low pressure of hydrogen in the system and a slow rate of temperature increment.   The TPR spectrum of evacuated CuY is shown by the broken curve in Fig. 3.   It coinsists of two
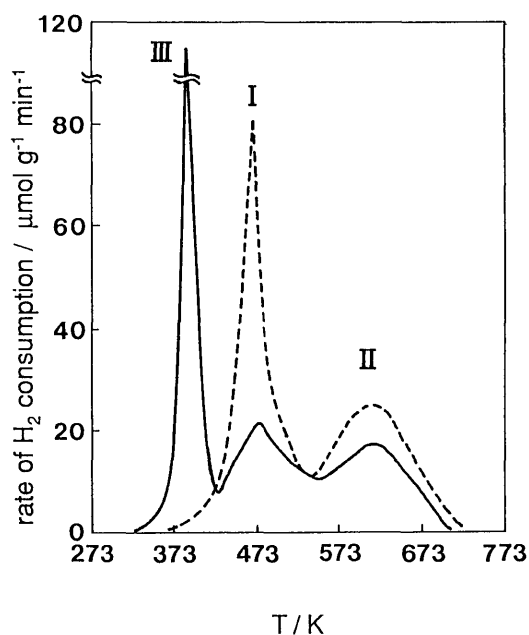
Fig. 3   TPR spectra for CuY with (solid curve) and without (broken curve) the R-O treatment (evacuated at 523 K, reduced at 673 K and reoxidized at 473 K).

distinct peaks with maxima around 470 and 630 K. The first peak (I) is associated with the reduction of Cu^{2+} to Cu^+ ions, while second maximum (II) suggests that of Cu^+ ions to Cu metal. This process was substantiated by the color changes of the sample during TPR experiment, i.e., the greenish blue sample turned white when the first maximum was observed, and then it turned pink above 650 K.

In order to confirm the changes of Cu species during the two-step reduction, ESR measurements were carried out for the sample after each step in the TPR precess (Fig. 4),i.e., after dehydration at 523(a), reductions at 523(b) and 673 K (C). The dehydrated sample shows a broad symmetric signal (Fig. 4a).
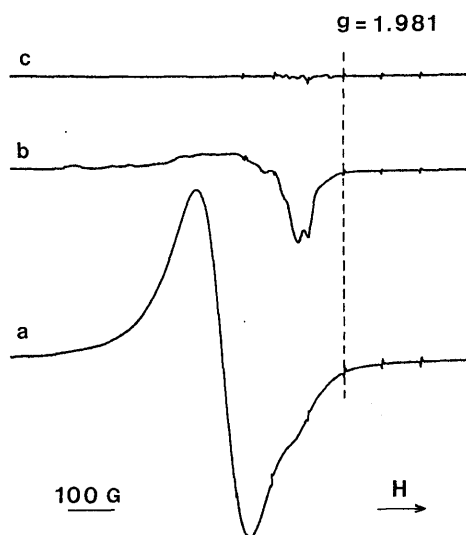
Fig. 4 ESR spectra of (a) original CuY, (b) reduced CuY at 523 K, and (c) reduced CuY at 673 K.

The g value and line width of dehydrated CuY was 2.17 and 117 Gs, respectively. It has been attributed to nonlinear pairs of Cu^{2+} ions undergoing spin-exchange interactions,[22] since more than two Cu^{2+} ions are considered to present in the sodalite cage in the present sample. It is considered that the broad symmetric signal of CuY dehydrated at 523 K is due mainly to two kinds of configurations around Cu^{2+} ions. Cu^{2+} ions exchange electrons with each other.[23] The observed spectrum indicates the existence of ion pairs in the sodalite unit,as suggested by Chao and Lunsford.[22] A small asymmetric peak associated with isolated Cu^{2+} ions was observed in Fig. 4a. It was speculated that there are small portion of isolated Cu^{2+} ions in the small cages after the evacuation at 523 K.

The ESR spectrum of CuY sample reduced at 523 K in the mode of TPR showed asymmetric signal, as shown in Fig.4b. The intensity and shape of spectrum shown in Fig. 4b is very similar to that of CuY with low copper con-

tent.[24]   It is associated with the isolated Cu^{2+} ions located in the hexagonal prisms, where the reduction is difficult to occur at low temperatures. Therefore, small portion of Cu species in zeolite still remain as Cu^{2+} ions by the reduction at 523 K.

After reduction of the sample at 673 K no ESR signal was observed in the spectrum (Fig. 4c).   It is suggested that Cu^{2+} ions were almost reduced to Cu^+ ions or Cu metal.   During the TPR process, the amounts of hydrogen consumed at 573 and 723 K were estimated to be 0. 49 and 0. 85 mole atom-Cu^{-1}, respectively.   These values suggest that all Cu^{2+} jons are practically reduced to Cu^+ ions by the TPR treatment up to 573 K.   Furthermore, Cu ions could not be reduced completely to metallic copper even at 723 K by the TPR process examined in the present study, as is indicated by the hydrogen consumption.

In order to check the formation of Cu^+ ions in the zeolite IR spectra were measured during the TPR process.   CO has been recognized to adsorb selectively onto Cu^+ ions and form $Cu^+ - CO$ complexes in the super cages.[25] Upon adsorption of CO, IR spectra of CuY were measured at each step during the TPR process (Fig. 5). Cu^{2+} ions in the evacuated sample is considered to be reduced into Cu^+ ions since a strong absorption band appeared at 2160

2800   2400   2000   1800
wavenumber / cm^{-1}
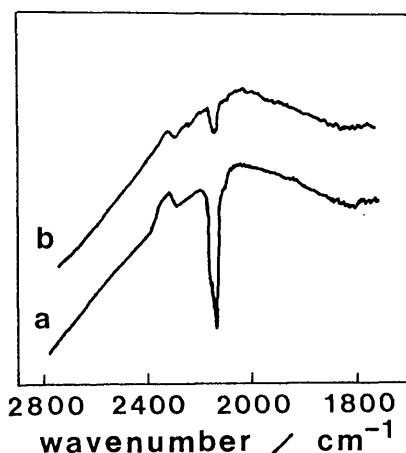
Fig. 5   IR spectra of Cuy during reduction process. A, CuY with reduction at 523 K;B, CuY with reduction at 473 K.

cm^{-1} due to Cu^+ complex.   It has been confirmed from these observations, thus, that Cu^{2+} ions in the zeolite are reduced into Cu^+ ions at 470 K, where the peak I is observed in the TPR spectra (Fig. 3).

After reduction at 673 K the band due to $Cu^+ - CO$ complex almost disappeared from the spectrum, as shown in Fig.5b.   In daaition, no signal of Cu^{2+} ions were observed in the ESR spectrum after reduction at 673 K.   Therfore, Cu^+ ions were transformed into Cu upon reduction at 673 Kin TPR. However, a little peak still remained in IR spectrum after reduction at 673 K

(Fig. 5). It was considered that small portion of Cu^+ ions were remaind in small cavity such as site I in zeolite Y.

When the CuY with consecutive reduction-reoxidation (R-O) treatment was reduced at 473 K, a new peak (III) appeared around 390 K in the TPR spectra, as shown by the solid curve in Fig. 3. The total hydrogen consumption throug h this TPR was 1.07 mmole g-CuY^{-1}. The hydrogen consumed for the peak III was 0.49 mmole g-CuY^{-1}. Therefore, about 46% of original Cu^{2+} ions was transformed into the easy-reducible species X by the R-O treatment. Thus, active Cu species formed in the zeolite during this treatment.

The formation of species X depends remarkably on the temperatures of each stage in the R-O treatment, such as peliminary evacuation, reduction with hydrogen and reoxidation with oxygen. Figure 6 A depicts the effect of evacuation followed by reduction and reoxidation under the standard condition at 673 K for 2 h. With the increase in vacuation temperature, the
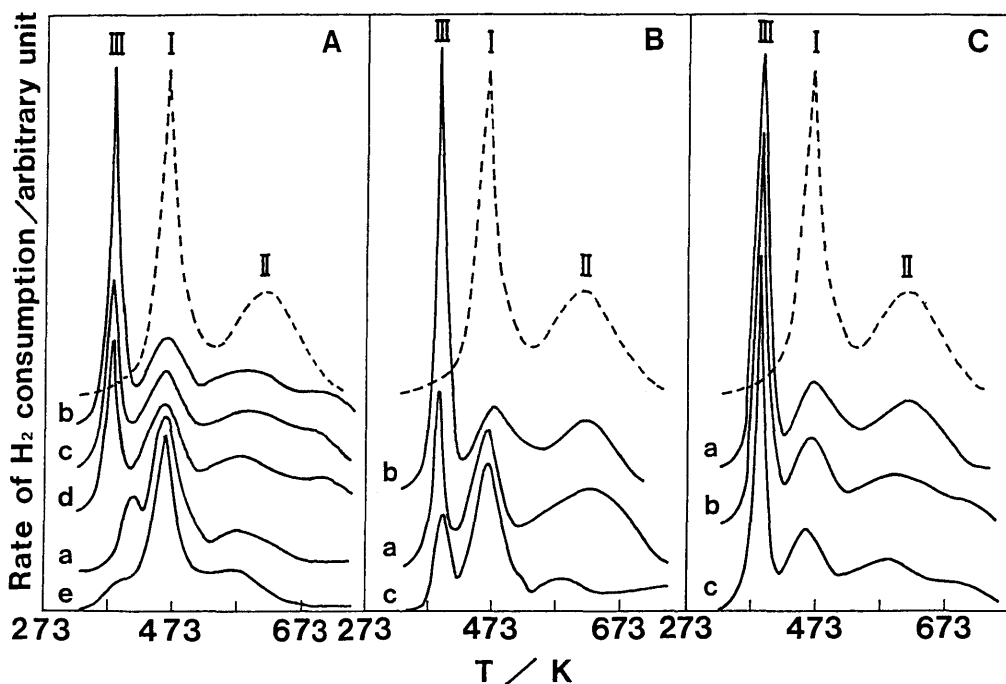
Fig. 6   TPR spectra of CuY with the R-O treatment under various conditions. A; CuY evacuated for 0.5 h at (a) 293, (b) 523, (c) 573, (d) 673, and (e) 773 K (reduced for 2 h at 673 K and reoxidized for 2 h at 673 K). B; CuY reduced for 2 h at (a) 573, (b) 673, and (c) 773 K (evacuated for 0.5 h at 523 K, and reoxidized for 2 h at 473 K).C; CuY reoxidized for 2 h at (a) 473, (b) 573, and (c) 673 K). Broken curve, CuY without the R-O treatment.

amount of species X remarkably decreased, whereas those of peaks I and II increased in the TPR spectra.   The amount of hydrogen consumption for the peak III decreased with the increase in the evacuation temperature.   The total hydrogen consumption during TPR process, furthermore, decreased with the increase in evacuation temperature.   It is indicated, therefore, that a great portion of Cu^+ ions in the zeolite evacuated at higher temperatures remained unchanged in the TPR procedure up to 773 K, as suggested by Gentry et al.[28]

The effect of reduction stage in the course of the R-O treatment is shown in Fig. 6B. The maximum formation of species X was observed by the reduction at 673 K.   In the case of reduction at lower temperatures a great portion of Cu species in the zeolite remained as Cu^+ ions.   Upon the following reoxidation with oxygen, these Cu^+ ions were probably reoxidized back to Cu^{2+} ions located at the original lattice positions.[26]   Therefore, the formation of Cu metal, which prevents such reversible redox cycle, is considered to be necessary in the formation of species X.   The reoxidation stage during the R-O treatment, on the other hand, scarcely affects on the formation of species X, as shown in Fig.6C.   The intensity of the peak III slightly decreased with the increase in the reoxidation temperature.   In the temperature-programmed oxidation of the sample reduced at various conditions, only one sharp peak was observed at a low temperature around 470 K, indicating a high velocity of the reoxidation stage in this system.

Among each stage in the R-O treatment, as described above, the evacuation stage showed the most significant influence in the formation of species X, i.e., the lower temperature in the evacuation stage, the more preferential it is for the formation of species X.   It is speculated from this point of view that a small quantity of water is needed for a preferential condition of the following reduction stage.   It has already been recognized[29, 30] that small amounts of water is still adsorbed on the zeolitese vacuated at lower temperature. Recently, Sano et al.[31]   recognized the remarkable effect for reduction of hydrated staten NiY-NaOH system.   It has bee reported by Naccache et al.,[32] furthermore, that the reduction of Cu^{2+} ions in CuY is promoted in the presence of water via the formationof $Cu(OH)^+$ ions as the intermediate.   The role of water in the present work was qualitatively confirmed by the introduction of water to the system.   For example, when in the reduction stage 2.0 kPa of water was introduced onto the sample evacuated at 773 K, the amount of species X formed after the R-O treatment increased from 0.05 to 0.40 mmole g^{-1}, as is shown in Fig. 7.

The hydrogen consumpion of CuY zeolite with various conditions in the
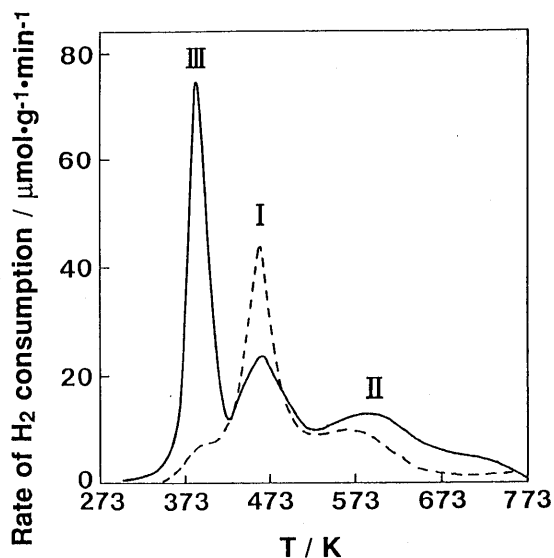
Fig. 7 TPR spectra for the activated CuY (evacuated at 773 K, reduced at 673 K and reoxidized at 673 K) in the presence (solid curve) and absence (broken curve) of water during the reduction stage.

evacuation, reduction, and reoxidation stages were summarized Table 1. It was concluded that the optimum conditions of the evacuation, reduction and reoxidation stages were 523, 673 and 473 K, respectively.

Table 1 Effects of temperature of evhcuation, reduction and rexidation stages during the R-O treatment on the formation the active species X.

| | temperature/K | | | H_2 consumption/mmol g^{-1} | |
	evac.*1	redn.*2	oxin.*3	species X	total
effect of evacuation	293	673	673	0.12	0.75
	523	673	673	0.38	0.97
	573	673	673	0.27	0.94
	673	673	673	0.22	0.91
	773	673	673	0.05	0.62
effect of reduction	523	573	673	0.19	1.08
	523	673	673	0.49	1.07
	523	773	673	0.15	0.79
effect of reoxidation	523	673	473	0.49	1.07
	523	673	573	0.49	1.06
	523	673	673	0.38	0.97

Each step during the treatment was performed for *1, 0.5h; *2, 2h; *3, 2h.

Structure of CuY zeolite during TPR Process

It is considered that the species X is expected to function as the catalytic centers in the oxidation reaction since it is readily reduced at low temperature (390 K) by hydrogen. The questions are why active species is formed by the R-O treatment and what is the chemical entity of the species X. The structural changes of Cu species during R-O treatment have been observed preliminarily by the XRD spectroscopy to resolve the questions. After reduction of the sample at 673 K, the weak diffraction pattern due to Cu metal was observed in XRD spectrum. Petunchi et al.[33] and Miro et al.[34] have already recognized in XRD measurements that large CuO crystals are formed in the oxidized Cu-zeolites after cyclic treatments with CO and O_2 at a high temperature of 1023 K. However, the XRD pattern of CuO crystals could not be observed in CuY with the R-O treatment in the present work. It has generally been known that the particles smaller than 50 Å doesn't show distinct diffraction patterns.

The EXAFS measurements have been performed for each step during the TPR process in order to investigate the structural changes of CuY zeolite with and without the R-O treatment. The normalized observed spectra and extracted oscillations for CuY zeolite in each stage during the R-O treatment, such as evacuation, reduction and reoxidation, are shown in Figs. 8A, B and C, respectively. The EXAFS oscillations for CuY without the R-O treatment during the first reduction process are shown in Figs. 9A, B and C. Furthermore, the EXAFS spectra during the TPR process of the sample with the R-O treatment are shown in Figs. 10A, B and C in the similar way. In Figs. 11 A, B and C the EXAFS oscillations for reference materials, such as CuO, Cu_2O powders, and Cu foil are represented, respectively. Analysis of EXAFS spectra were carried out by Fourier transformation of the k^3-multiplied oscillations from k to R space. The radial distribution functions of CuY during R-O treatment obtained by Fourier transformation, are shown in Figs. 12-15. The peak positions in these radial distribution functions are about 0.3 Å smaller than true interatomic distances because of the phase shift.

In order to discuss the details of the structural basis of these species, furthermore, inverse Fourier transforms are carried out for the predominant peaks in each radial distribution function to determine the structural parameters, such as Debye Waller factor σ, interatomic distance R and coordination number of Cu atoms N. The inverse Fourier transforms are compared with the calculated values of $k^3\chi(k)$ assuming the Cu-O or Cu-Cu scattering
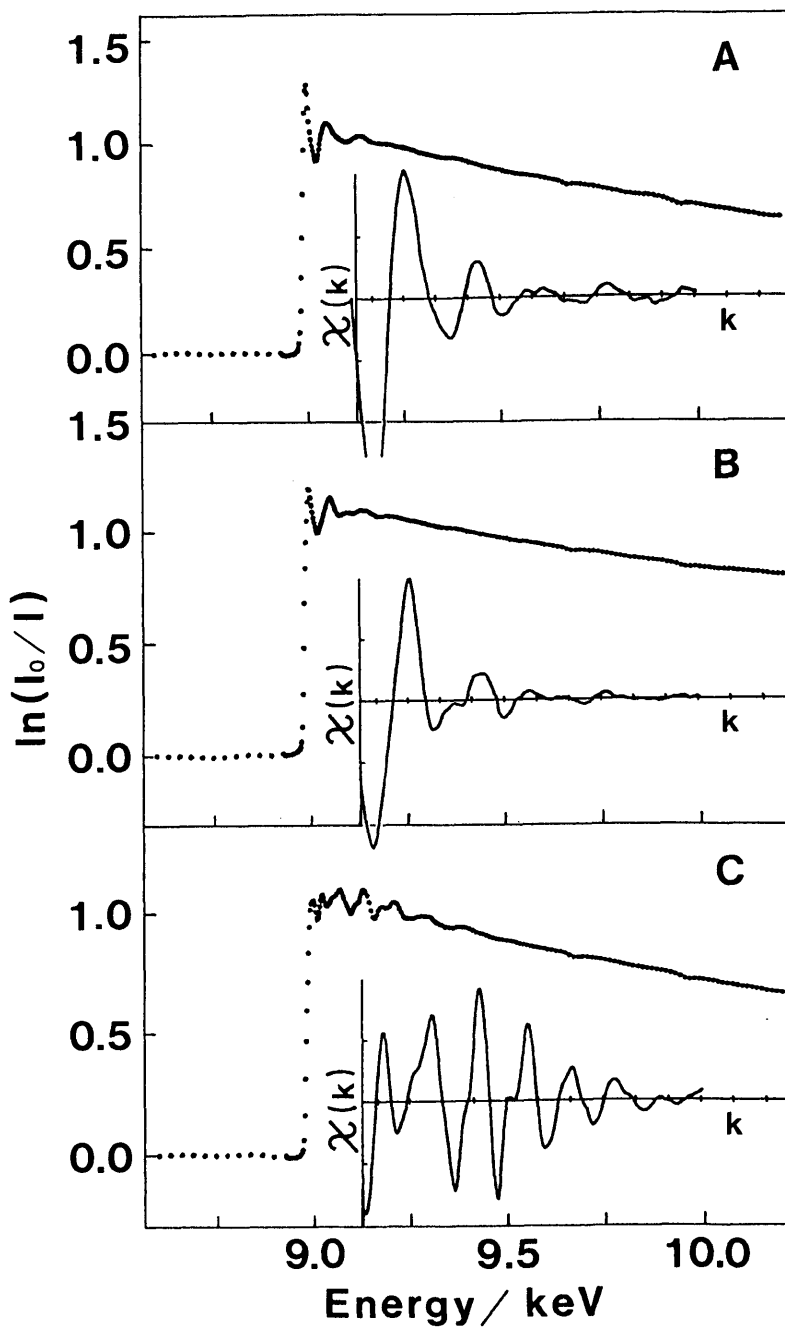
Fig. 8   The nomalized spectra and extracted oscillations of EXAFS for CuY.   A, CuY
with the evacation; B, the sample after redution of （A） with hydrogen; the
sample after reoxidation of （B） with oxygen.
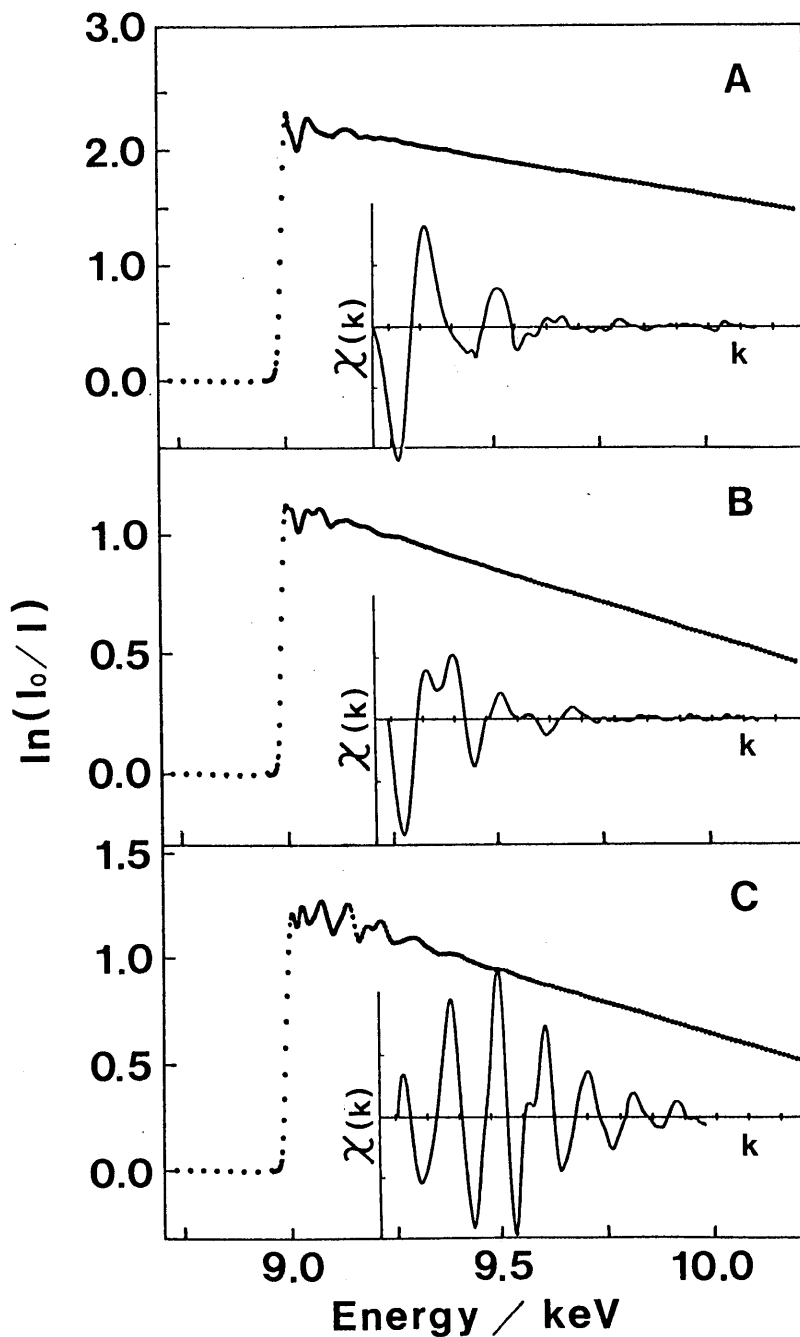
Fig. 9 The normalized spectra and extracted oscillations of EXAFS for CuY during re-
    dction process in R-O treatment. (A), CuY with the redution at 423 K; (B),
    reduction at 523 K; (C), reduction at 673 K.
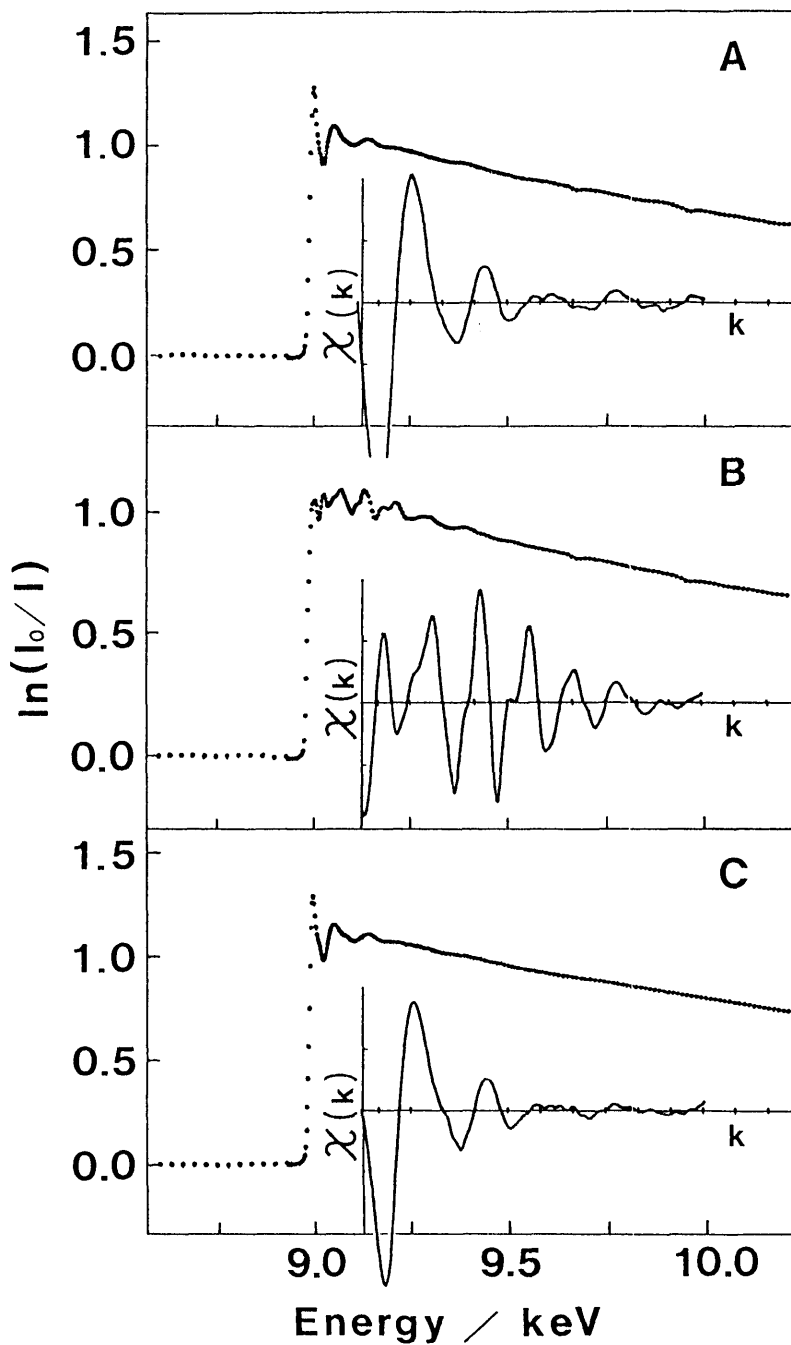
Fig. 10   The normalized spectra and extracted oscillations of EXAFS for CuY during redution process after R-O treatment.   (A), CuY with the reduction at 423 K; (B), reduction at 523 K and (C), reduction at 673 K.
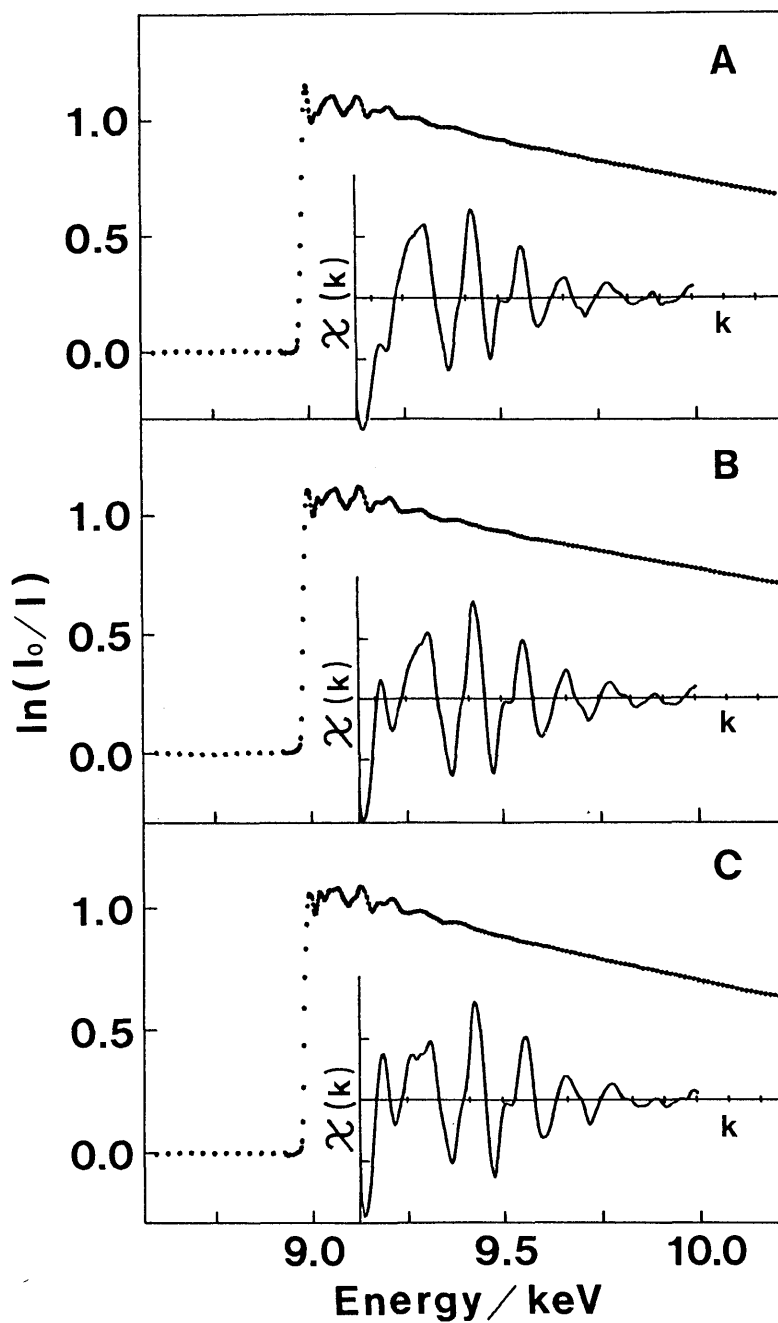
Fig. 11 The normalized spectra and extracted oscillations of EXAFS for reference materials. (A), CuO powder; (B), Cu₂O powder; (C), Cu foil.
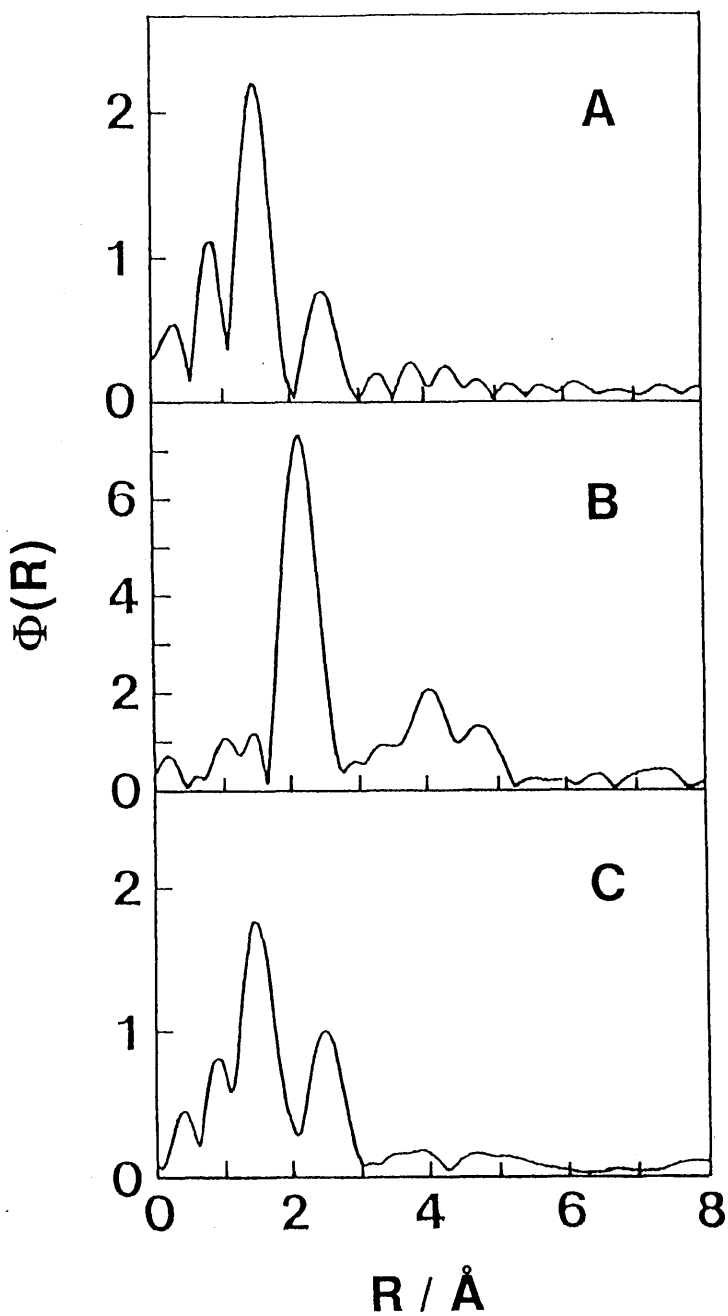
Fig. 12   Fourier transforms of EXAFS spectra for CuY during the R-O treatment on the sequence of (A) evacuation at 423 K (B), reduction at 673 K (C), and reoxidation
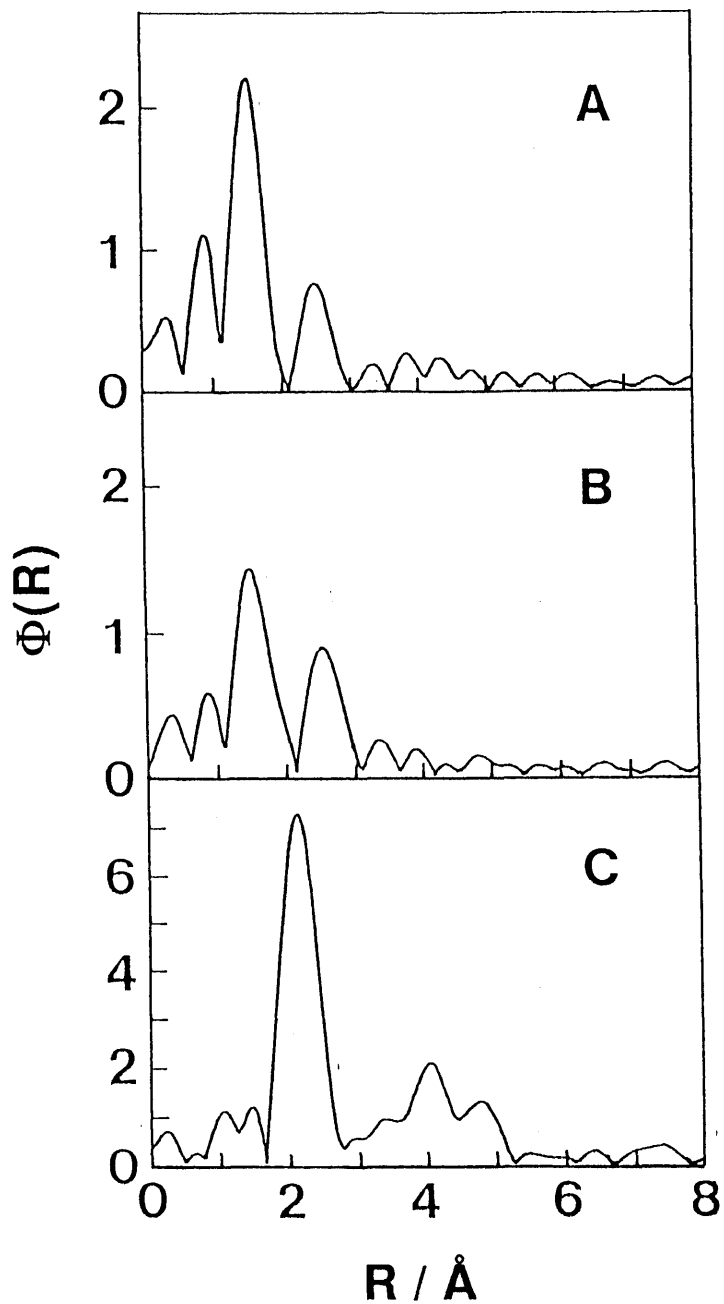
Fig. 13 Fourier transforms of EXAFS spectra for CuY without the R-O treatment in the course om TPR process.   Reduction temperature; 423 K (A), 523 K (B) and 673 K (C).
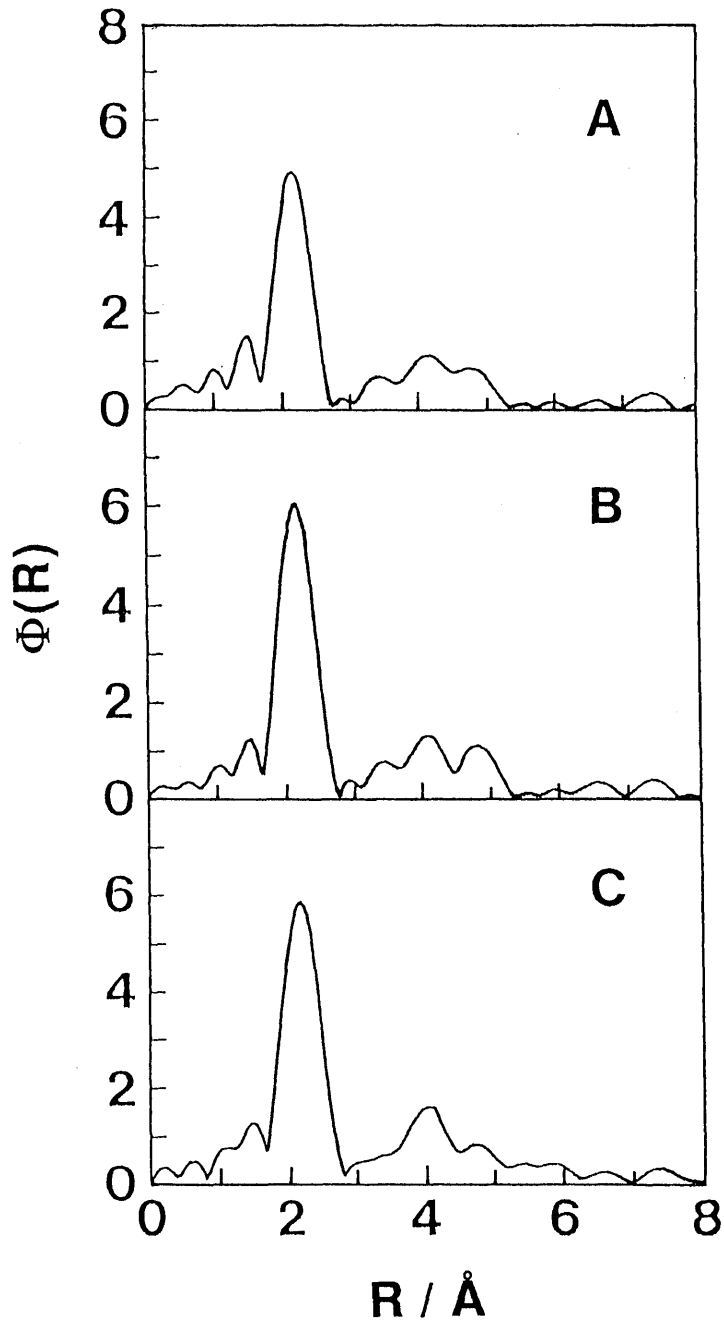
Fig. 14   Fourier transforms of EXAFS spectra for CuY with the R-O treatment in the course of TPR precdss.   Reduction temperature; 423 K (A), 523 K (B), and 673 (C).
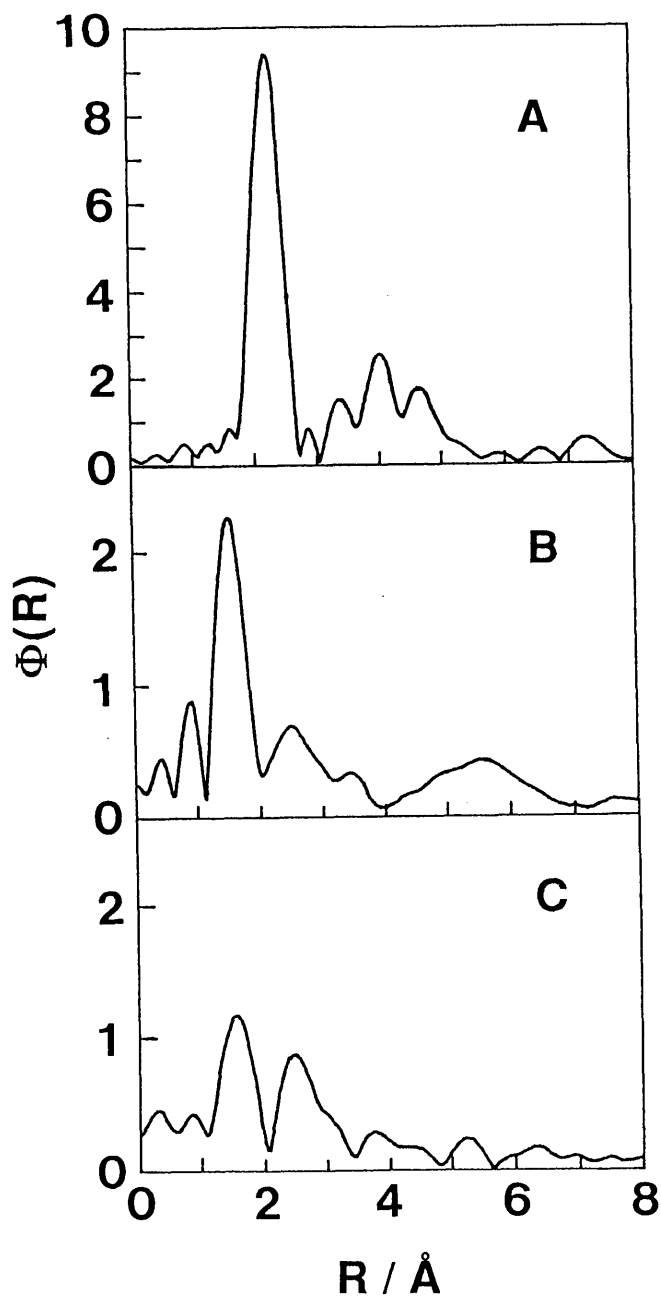
Fig. 15 Fourier transforms of EXAFS spectra for （A）Cu foil, （B）CuO powder and （C）Cu₂O powder.

Table 2 Best-fit values of structural parametrs on CuY zeolite with and withous the R-O treatment during TPR process.

sample	redn. temp./K	bond	σ	R/Å	N
	-	Cu-O	0.001	1.97	3.7
CuY without the	423	Cu-O	0.001	1.97	3.7
R-O treatment	523	Cu-O	0.002	1.93	2.8
	673	Cu-Cu	0.008	2.51	10.0
	-	Cu-O	0.000	1.96	4.4
CuY with the	423	Cu-Cu	0.008	2.52	7.0
R-O treatment	523	Cu-Cu	0.008	2.52	8.5
	673	Cu-Cu	0.008	2.52	8.8
Cu foil	-	Cu-Cu	0.008	2.51	12.0
CuO powder	-	Cu-O	0.002	1.96	4.0
Cu2O powder	-	Cu-O	0.001	1.86	2.0

obtain the "best-fit" curves.   These results are summarezed in Table 2.

The distance (R) of the Cu-O bond in evacuated sample shows 1.97 A (Fig. 12A).   This value approximately corresponds to the distance between Cu^{2+} ions at site I'position and lattice oxygen atoms in the sodalite cages of Y-zeolite.[4]   The coordination number of Cu atoms in 59.6% exchanged CuY used in this study is determined to be $N=3.7$.   Gallezot et al. reported in the XRD study that a greater portion of Cu^{2+} ions in 54% exchanged CuY zeolite were located at site I' in the sodalite cages.   The site I' Cu^{2+} ions are co-ordinated with three oxygens.   The coordination number of Cu^{2+} ions in the present sample is $N=3.7$, which probably indecates an average value between bare ions and hydrated ions in the sodalite cages.

After the evacuated sample is reduced with hydrogen at 673 K for 2 h, a strong peak observed at 2.51 A in the radial distribution function(Fig. 12B), which is coincides with the Cu-Cu bond in Cu foil (Fig. 15A).   However, co-ordination number of Cu atoms in reduced CuY ($N=10.0$) are slightly smaller than that of Cu foil ($N=12.0$).   It is indicated in the hydrogen consumption that most Cu^{2+} ions in the zeolite evacuated at 523 K has been reduced into Cu metal.   Petunchi et al.[33]   and Gentry et al.[28]   reported, however, that Cu^{2+} ions in the Y-zeolite were reduced with hydrogen into Cu^{+} ions.   The incompletion of reduntion in these studies is probably attributed to the absence of adsorved water in the zeolite matrix, as described before, since in their experiments the zeolite was treated at elevated temperatures above 773 K prior to the measurements.

After the R-O treatment, radial distribution function shows the main peak associated with Cu-O distance (Fig. 12C). Herman et al.[26] have reported that the Cu metal particles on the internal surface of the zeolite are reoxidized back to Cu^{2+} ions located at the original sites. In order to examine the structure of CuY after R-0 treatment, ESR spectra have been measured and the results are shown in Fig. 16. The peak intensity due to Cu^{2+} ions of the
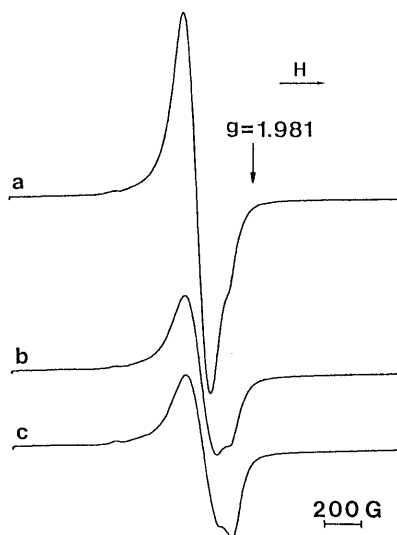
Fig. 16 ESR spectra for CuY with various treatments . a, original CuY ; b, Cu Y with the R-O treatment; and c, the sampl e a fte r reduction of (b) with H_2 at 423 K.

sample after R-O treatment (b) was extremely smaller than that in the original CuY (a). Furthermore, when the CuY with the R-O treatment was reduced at 390 K, the intensity of ESR signal remained unchanged although the peak Ⅲ was completely eliminated from the TPR spectrum. It is indicated from this observation that the species X has to be non-paramagnetic. Therefore, ESR-insensitive species such as CuO or Cu_2O probably formed in zeolite matrix after the R-O treatment. From Table 2, the Cu-O distance in CuO (1. 86 Å) is much shorter than that inspecies X(1. 96 Å), which well coincides with that in CuO(1. 96 Å). The extracted oscillations of CuY after R-O treatment, CuO, and Cu_2O are compared in Fig. 17. The EXAFS oscillation of CuY with R-O treatment bears closer resemblance with that of CuO rather than that of CuO. Furthermore, the calculated curve for the main peak (Fig. 12C), assuming the Cu-O scattering in CuO, well reproduces the inverse Fourier transforms for the samplewith the R-O treatment (Fig. 18A). Therefore, the species X can be assigned to CuO. In the TPR spectrum under the similar conditions CuO on SiO_2 showed a single broad peak around 420 to 470 K, while the species X showed a sharp peak at 390 K.
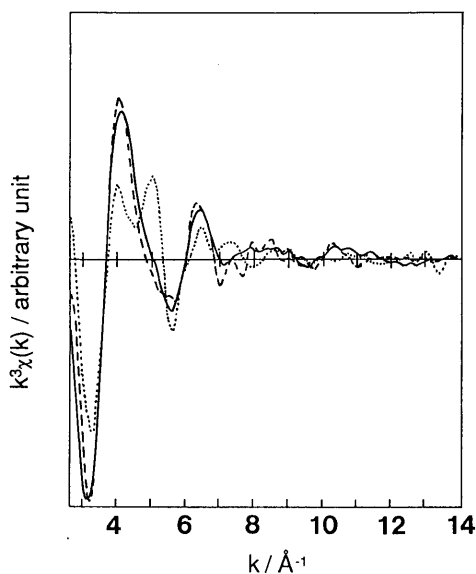
Fig. 17 Comparisons of extracted oscillations of the observed EXAFS spectra for CuY with the R-O treatment (solid curve), CuO powper (broken curve) and Cu_2O powder (dotted curve).

After reduction of CuY with the R-O treatment at 423K, the peak III has been eliminated from the TPR spectra (Fig. 3).   When the reoxidized CuY was again reduced with hydrogen at 523 K(Fig. 14A), the radial distribution function shows the peak due to the Cu-Cu bond distance in Cu foil.   The calculated curve for the main peak in Fig. 14A, assuming the Cu-Cu scattering in Cu metal, reproduces completely the obtained inverse Fourier transforms, as is depected in Fig. 18B.   It means that Cu species in the CuY zeolite with
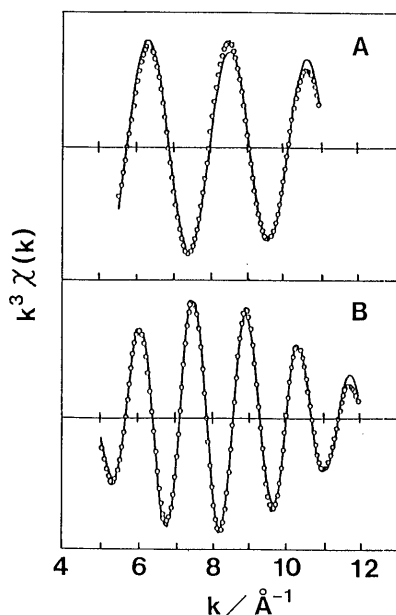
Fig. 18 Comparisons of the inverse Fourier trausforms (solid curves) with the "best-fit" values (circles) calculated assuming the Cu-O and Cu-Cu scatterings. A, CuY with the R-O treatment; and B, the sample after reduction of (A) with CO.

the R-O treatment were directly reduced with hydrogen into Cu metal at a considerable low temperature.   It demonstrates the dramatic influence of the R-O treatment, since in the case of the original CuY no changes are observed in the EXAFS and TPR experiments by the reduction at this temperature. Thus, the TPR peak around 390 K can be assigned to direct reduction from CuO clusters to Cu metal, while the original Cu^{2+} ions in the zeolite are reduce at higher temperatures by the two-step mechanism, via Cu^+ ions to Cu metal.

In the Fourier transforms shown in Fig. 14A, however, intensity of the peak associated with the Cu-Cu distande in Cu metal was quite smaller than that in Cu foil.   The discrepancy between these values is mainly attributed to the difference in the size of Cu metal,[35, 36] i.e., the coordination number in small particles is smaller than that in large crystals because of the high proportion of surface atoms.   Applying the theory by Greegor and Lytle[37] to the present system and assuming the spherical particle shape of Cu metal, the average size of the Cu clusters is roughly estimated to be 6 - 8 Å.   This size of particle is distinctly smaller than the main cavity size of the faujasite framework (ca.12 Å) and so small as to escape XRD and TEM observations.

Catalytic properties of CuY zeolite with R-Otreatment in CO oxidation

In order to obtain an information about the catalytic activity of CuY with the R-O treatment, the reaction of CO oxidation has been carried out in the circulation system at low temperatures.   The original CuY showed no appreciable activity for CO oxidation reaction at 373 K, as shown iby thd droken curve in Fig. 19.   On the other hand, the CuY after the R-O treatment under
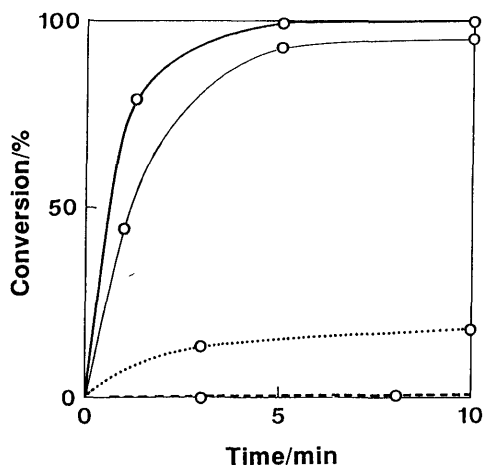
Fig. 19   Plots of CO conversion versus time on CuY with various treatments. Thick curve, CuY with the R-O treatment; dotted curve, CuY with redution; broken curve, fresh CuY; and thin curve, $CuO-SiO_2$ catalyst.

an appropriate condition showed high activity (solid curve) and exceeded that of aconventional CuO/SiO₂ catalyst.   Although reduced CuY (without the reoxidation step) started in an extremely low activity (dotted curve), however, its activity increased very slowly but continuously with time on stream of the reactant.   Figure 20 indicates the TPR traces of the sample after the usage
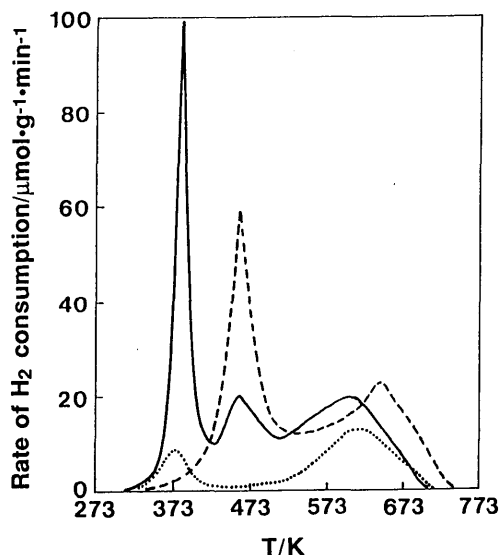
Fig. 20   TPR spectra of CuY during CO oxidation reaction. Solid curve, CuY with the R-O treatment; broken curve, fresh CuY; dotted curve, reduced CuY.

in the CO oxidation for 1 h at 373 K.   The original CuY (broken curve) showed the similar spectrum to that before catalysis (Fig. 3).   In the TPR spectrum for the sample with the R-O treatment (solid curve), the peak Ⅲ showed no appreciable decrease incomparison with that before catalysis (Fig. 3).   After the usage in CO oxidation, on the other hand, a small peak III was observed in the TPR spectra for the reduced CuY (dotted curve).   It is indicated from these observations that the active species were forming gradually on the reduced CuY zeolite in the oxidative circumstance of the reactant stream of CO in oxygen.

   In order to investigate the relationship between the rate of CO oxidation and the amount of the species X, the reaction has been carried out at low temperatures using a conventional flow system connected with the circulation system.   The computation of rates in the CO oxidation at the steady state is simplified by the low conversions used in the differential reactor.   The corresponding high gas velocity through the bed and small particle size of catalys t ensure that there are no transport limitations.   As shown in Fig. 21, good straight lines were obtained upon plotting the CO conversion (X) against the time factor(W/F).   The rate of CO oxidation (r), therefore, can be determined by the equation of $r = x\ W^{-1}\ F$, where W and F are the amount of CuY used
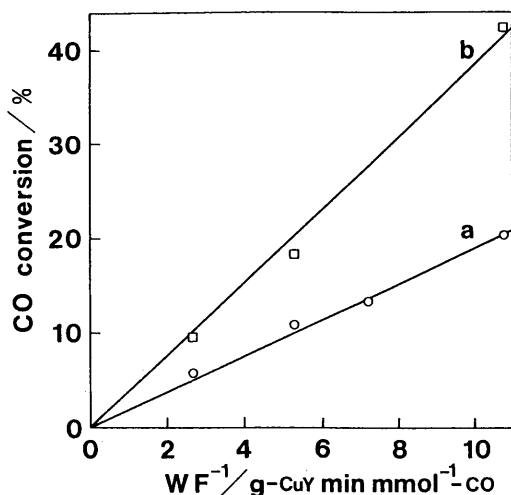
Fig. 21 Relation between CO conversion and time factor (a) at 393 and (b) 413 K.

and the flow velocity of CO through the catalyst bed, respectively.

In order to check the catalytic action of species X, the rates of CO oxidation reaction were measured on CuY with R-O treatment under various conditions.   The rates of CO oxidation are plotted against the amounts of species X obtained from the area of peak Ⅲ of the TPR spectra in Fig. 6.   The results at 373 and 393 K are shown in Fig. 22.   The rates of oxidation at these tem-
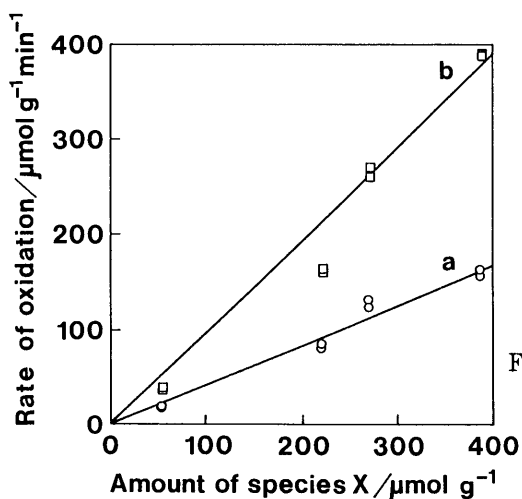
Fig. 22 Dependence of catalytic activity on the quantity of species X at (a) 373 and (b) 393 K.

peratures increases proportionally with increasing in the amount of species X.   Therefore, it is expected that the species X can function as the catalytic centers for CO oxidation reaction.

Figure 23 shows the Arrhenius plots of the rate in the CO oxidation on
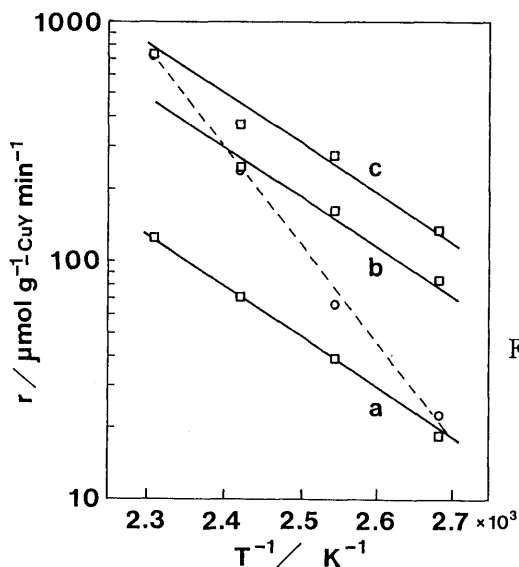
Fig. 23 Arrhenius plots of CO oxidation on CuY with varivus amounts of species X. a, 0.05; b, 0.22; and c, 0.27 mmole g^{-1}. Broken line, CuO-SiO_2.

the CuY with various amounts of the species X (solid curves), together with that on the conventional Cu/SiO_2 catalyst (broken curve). The data show excellent linear relationships. From the slopes of these plots, the apparent activation energy of the reaction catalyzed by CuY zeolite with the R-O treatments is estimated to be 42 kJ mol^{-1} which is virtually independent of the amount of the species X on the surface. It probably indicates a homogeneity of active species formed, as is expected from the sharp peaks III at the same temperature in the TPR spectra (Fig. 6). That is, the R-O treatment under various conditions changes not quality but quantity of the active species X. Furthermore, the activation energies of CuY with the R-O treatment was extremely lower than that of CuO/SiO_2 catalyst (81 kJ mol^{-1}).

Structural changes of CuY during the catalysis

In order to investigate the catalytic behavior of CuY with the R-O treatment during the CO oxidation reaction, a cyclic treatment with CO and oxygen has been carried out at the reaction temperature of 423 K. The TPR spectra of the sample during the redox cycle are shown in Fig. 24. When the CuY sample after the R-O treatment (Fig. 24a) was treated with CO at the reaction temperature of 423 K, the peak III was completely eliminated from the TPR spectrum(Fig. 24b), indicating that the species X was reduced by CO at 423 K. Only formation of CO_2 was observed as the gaseous product in this CO
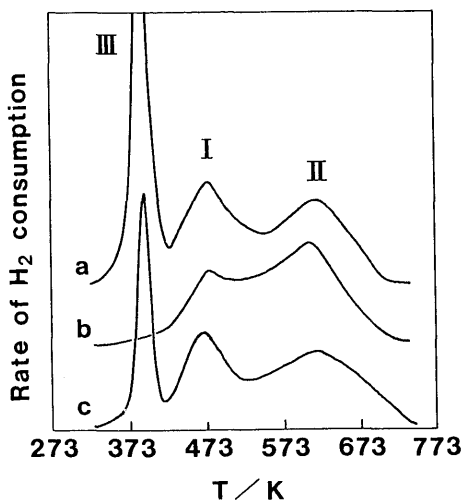
Fig. 24 TPR spectra for CuY with the R-O
treatment during the redox cycle.
a, CuY with the R-O treatmeut; b,
after reduction of (a) with CO;
and c, afser reoxidation of (b)
with O_2.

treatment.   When the CO-reduced catalyst was reoxidized with oxygen at the
same temperature, the peak III was reproduced, as shown in Fig. 24c, al-
though some decrease was recognized in its intensity.   It is attributed to the
incompletion of reoxidation because of the lower temperature in comparison
with that in the R-O treatment.   From these results, it is expected that the
redox reaction of the species X with CO and oxygen proceeds reversibly also
in the catalysis.

In order to confirm the structural changes of the sample during the redox
treatment with CO and oxygen, the EXAFS measurements were carried out
at each step in the cyclic treatment.   The observed EXAFS spectra and their
extracted oscillations in this experiments are shown in Fig. 25.

Figures 26A-D shows the Fourier transforms of the EXAFS spectra for
the catalyst in sequence of each step during the redox cycle with CO and
oxygen at 423 K.   The"best-fit" values of the structural parameters of these
sample obtained by the curve fitting are shown in Tabel 3.   When CuY with
the R-O treatment has been reduced with CO an intense peak appears at the
distance of R=2.52 Å (after the correction of the phase shift) in the radial
distribution function (Fig.26B).   This bond well coincides with the Cu-Cu
distance in Cu foil.   The inverse Fourier transforms of this peak completely
reproduces the calculated values from the Cu-Cu scattering in Cu metal, as
demonstrated inFig. 27B.   By the treatment with CO at the reaction tempe
rature, therefore, the species X is reduced directly into Cu metal, whereas the
original Cu^{2+} ions converts slowly into Cu^+ ions (at much higher temperatures
above 673K).
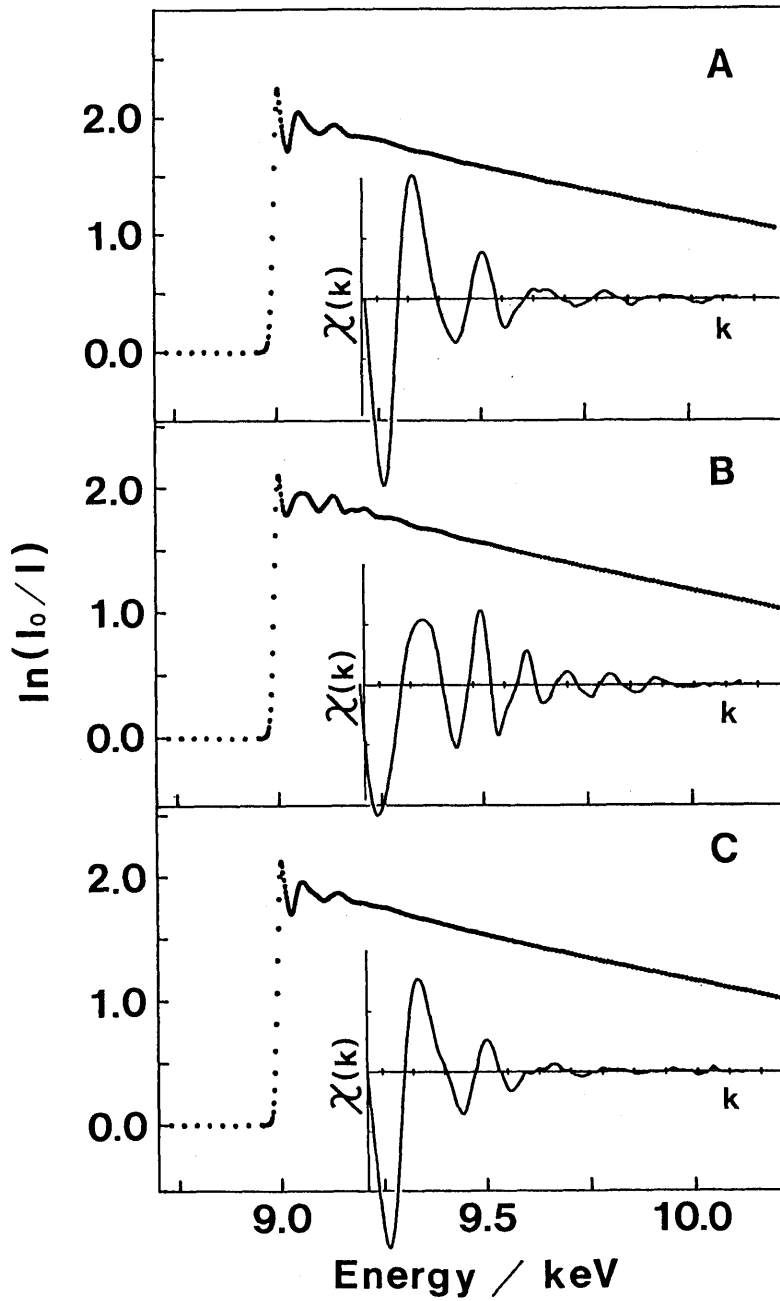
Fig. 25 The normalized spectra and extracted oscillations of EXAFS for CuY with the
R-O treatment during the redox cycle. (A), CuY with the R-O treatment; (B),
the semple after reduction of (A) with CO; and (C), the semple after reoxida-
tion of (B) with O_2.

Toble 3   Best-fit valtes of structuras parameters from EXAFS data in the sequence
          RgO treatment and catalysis.

sequence	sample and treatment	bond	σ	R/Å	N
1	evacuated CuY at 523 K	Cu-O	0.001	1.97	3.7
2	reduced (1) with H_2 at 673 K	Cu-Cu	0.008	2.51	10.0
3	oxidized (2) with O_2 at 473 K	Cu-O	-0.000	1.96	4.4
4	reduced (3) with CO at 423 K	Cu-Cu	0.006	2.52	5.0
5	oxidized (4) with O_2 at 423 K	Cu-O	0.003	1.96	4.2
6	reduced (5) with CO at 423 K	Cu-Cu	0.007	2.52	4.9
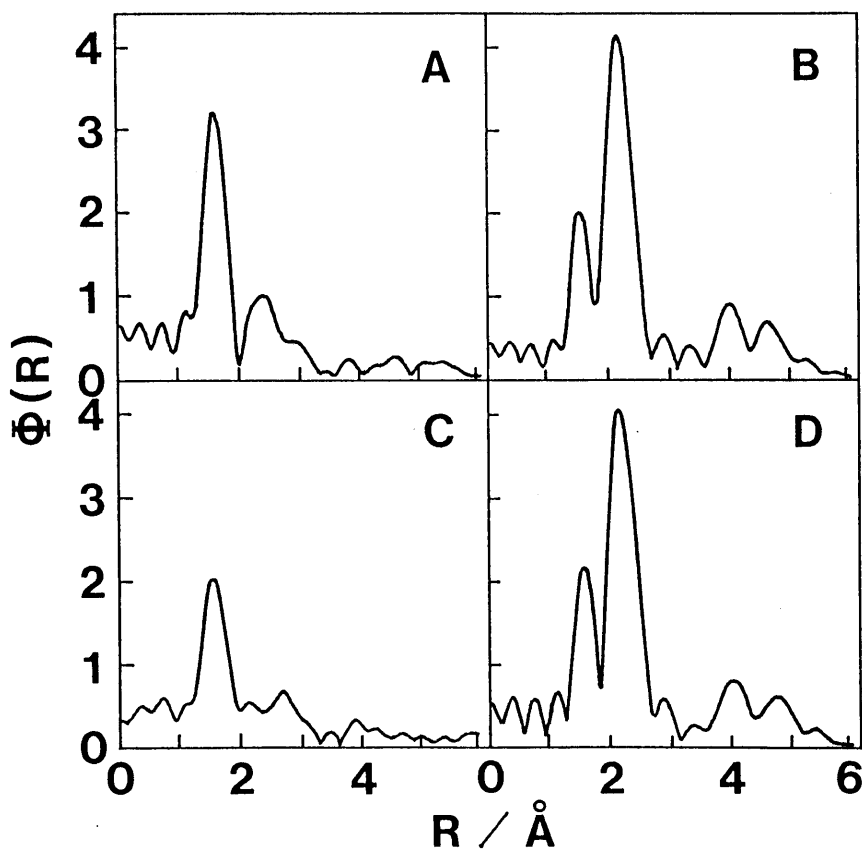
Fig. 26   Fourier transforms of EXAFS spectra for CuY with the R-O treatment during
          the redox cycle.   (A), CuY with the R-O treatment; (B), after reduction of
          (A) with CO; (C), the semple after reoxidation of (B) with O_2 ; and (D),
          after reduction of (C) with CO.
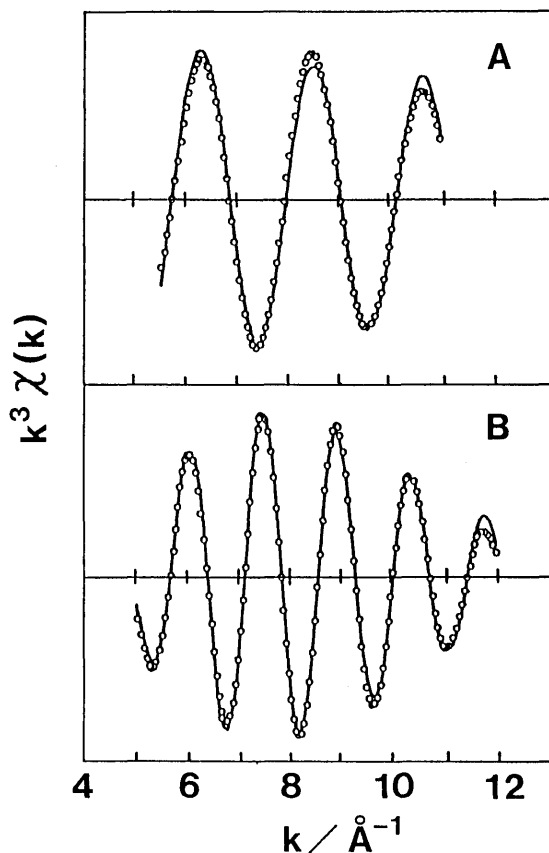
Fpg. 27   Comparisons of inverse Fourier transforms for the main peaks in Figs. 5-10 C
(A) and 5-24A (B) with best-fit curves assuming the Cu-O and Cu-Cu scatter-
ings, respectivlly.

In the subsequent reoxidation of this CO-reduced catalyst the predomi-
nant peak again appears at the Cu-O distance in the Fourier transforms, as
shown in Fig. 26C.   Upon the second CO-treatment of this reoxidized sample
(Fig. 26D), furthermore, it shows exactly the same radial distribution with
that upon the first CO-treatment (Fig. 26B).   In the redox cycle with CO and
oxygenat the reaction temperature, thus, the reversible behavior observed in
the Fourier transforms well agrees with the results in the TPR experiments
described in Fig. 24.

The coordination number in the metal formed from thespecies X by the
CO treatment (N=4. 9-5. 0) is extremely smaller than those in the hydrogen-
reduced sample (N=10. 0) and in the infinite crystal (N=12. 0).   The discrep-
ancy between these values is mainly attributed also to the difference in the
size of Cu metal.   According to the approximation by Greegor and Lytle,[37]

the size of Cu particles during in the redox cycle is roughly estimated to be 4 - 6 Å. In order to draw the active species more clearly, the size of the metal clusters for the species X has been estimated from the another point of view. First, the models of the metal clusters with various Cu atoms are drawn by a computer according to the close-packed structure, as shown in Fig. 28 which represents a typical example of ten-atoms cluster. Then, the number of Cu atoms osculating with a difinite atom is counted (the number of osculating atoms will corresponds to the coordination number of the definite atom). This counting is carried out for all atoms in the clusters with various Cu atoms. Finally, the sum of the number of osculating atoms for each cluster is divided by the number of Cu atoms in that cluster. The average number of osculating atoms will indicate the average coordination number of Cu atoms in the metal clusters. The results are shown in Fig. 29.
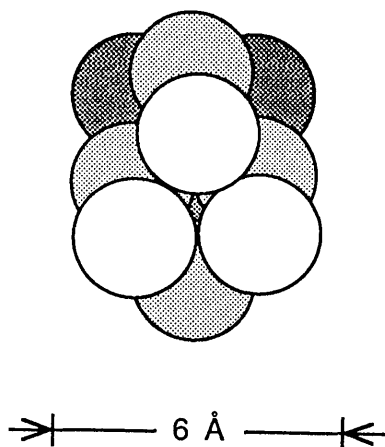
Fig. 28   Atypibal of Cu-metal cluster with ten atoms.
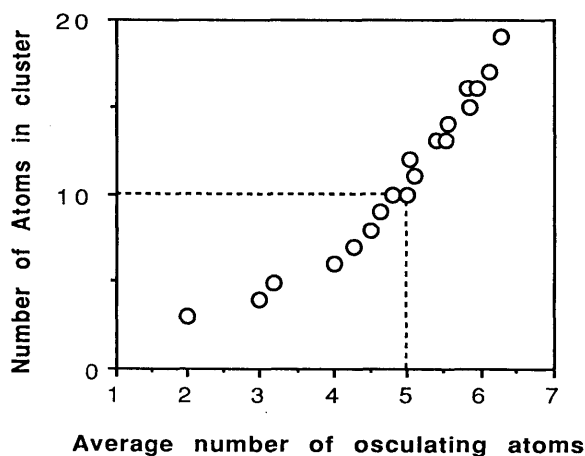
Fig. 29   The plot of average number of osculating atoms versus number of Cu atoms in the clusters.

The metal clusters formed by the CO-reduction of the species X shows the coordination number of N=4.9-5.0. This value corresponds approximately to that of the cluster with ten Cu atoms, as recognizd in fig. 29. Furthermore, the size of the ten-atoms cluster is estimated to be about 6 Å, which value well agrees with that calculated by the method of Gregor and Lytle (R= 4 - 6 Å).

As recognizd in Table 3, furtheermore, the coordonation number of Cu atoms in these metal clusters remeins unchaged thrugh the CO-oxygen redox

cycle.   It is speculated, therefore, that the number of Cu atoms in the species X is substantially retained during the CO oxidation reaction at the low temperature tested in this work.

From these observations describfed so far, the species X is plusible to be CuO clusters with several Cu atoms.   These clusters are reduced directly and reversibly with CO into metal clusters and function as the catalytic centers in the CO oxidation at the low temperature.

Conclusion

In the present study the redox and catalytic behavior of an activated CuY zolite have investigated and characterized mainly by the TPR and EXAFS measurements.   The results obtained are summarized here.

(1)   The formation of an active species X in the matrix of CuY zolite recognized in the observations by the TPR method.   The activation process consists of consecutive three stages in the sequence of preliminary evacuation, reduction with hydrogen and reoxidation with oxygen.   The maximum formation of the species X was observed at 523, 673 and 473 K, for these stages of the R-O treatment, respectively.

(2)   Analysis of the EXAFS data suggested that during the TPR process with hydrogen the species X was directly reduced into Cu metal at a low temperature, whereas the original Cu^{2+} ions in the Y-zeolite were reduced by a two-step mechanism, via Cu^+ ions into Cu metal crystals at high temperatures.

(3)   It was suggested from the kinetic measurements in the CO oxydation at low temperature that with the increase in the amount of the species X the rate of reaction increased proportionally, whereas the activation energy of reactions remaind unchanged.

(4)   It was elucidated from the EXAFS observations that in the treatment with CO the species X was directly reduced into Cu metal cluster at the reaction temperature, whereas the reduction of the original Cu^{2+} ions is restricted up to Cu^+ ions even at much higher temperatures.

(5)   Detailed calculation of the structural parameter indicated that the active species X was CuO cluster with ten Cu atoms on the average and that cluster size approximately 6 Å was retained during the reversible interconversion between CuO and Cu metal clusters.   As the conclusion point of view, the active species in this system is plausible to be small CuO clusters, which func-

tion as the catalytic center in the CO oxidation, via the reversible redox mechanism.

Acknowledgement

We express our gratitude to Drs. Y.Udagawa, K.Tohji and Mr .T.Mizushima (The Institute for Molecular Science, Okazaki, Japan) for their helpful supports in EXAFS experiments and analysis of the spectra.

Reference

a. H.Matsumoto and S.Tanabe, *J.Phys. Chem.,* in press,

b. H.Matsumoto and S,Tanaka, *J.Chem. Commun.,* **1989,** 875

c. S.Tanabe and H.Matsumoto, *Bull. Chem. Soc. Jpn.,* 63, 192 (1990).

d. S.Tanabe and H.Matsumoto, *Chem. Lett.* **1989,** 539.

e. S.Tanaka and H.Matsumoto, *Catalyst* 31, 353 (1989).

f. S.Tanabe and H.Matsumoto, *9th Int. Congr. Cryst. Gr.,* Sendai, p193 (1989).

g. S.Tanabe and H.Matsumoto, *Appl. Catal.,* **45,** 27 (1988).

h. S.Tanabe and H.Matsumoto, *Chem. Lett.* **1985,** 1425.

1. D.H.Olson, R.J.Mikovsky, G.F.Shipman, and E.Dempsey, *J.Catal.* **24,** 161 (1972).

2. I.E.Maxwell, J.J.de Boer, and R.S.Downing, *J.Catal.* **61,** 493 (1982).

3. M.J.Mortier, *"Compilation of Framework Sites in Zeolites",* Butterworth, Guildford, England (1982)

4. P.Gallezo, Y.Ben Taarit and B.Imerik, *J.Catal.* **26,** 295 (1972).

5. J.A.Rabo (ed.), *Am, Chem.Soc.Monogr* 171, (1976).

6. P.A.Jacobs *"Carboniogenic Activity of Zeolites."* Elsevier, Amsterdam, (1977).

7. P.B.Venuto, Catal.Org.Synth.Conf., 6 th, P. 67 (1977).

8. G.K.Boreskov, N.N.Bobrov, N.G.Maksimov, V.F.Anufrienko, K.G.Ione, and N.A. Shestakova Dokl.Akad.Nauk.SSSR, **201,** 887 (1971).

9. W.B.Williamson, D.R.Flentge, and J.H.Lunsford J.Catal., **37,** 258 (1975).

10. K.G.Ione, N.N.Bobrov, K.G.Boreskov, and L.A.Vostrikova, *Dokl.Akad.Nauk SSSR,* 210, 388 (1973).

11. G.K.Boreskov, *Proc.Int.Congr.Catal.,* 5th, 2, 981 (1973).

12. T.Kubo, H.Tominaga, and T.Kunugi, *Bull. Chem. Soc. Jpn.,* **46,** 3549 (1973).

13. N.G.Maksimov, K.G.Ione, V.F.Anufrienko, P.N.Kuznetsov, N.N.Bobrov, and G,K, Boreskov, *Dokl.Akad.Nauk. SSSR.* **217,** 135 (1974).

14. N.N.Bobrov, G.K.Boreskov, A.A.Davydov, and K.G.Ione, *Izv.Akad.Nauk SSSR,* Ser. Khim., 24, (1975).

15. K.G.Ione, N.N.Bobrov, and A.A.Davydov, *Kinet.Katal.* **16,** 1234 (1975).

16. R.A.Schonheydt, P.J.Vandamme, P.A.Jacobs, and J.B.Uytterhoeven, *J.Catal.*, **43**, 292 (1976).

17. R.L.Garten, W.N.Delgass, and M.Boudart, *J.Catal.*, **18**, 90 (1 970).

18. R.AA.Dalla Betta, R.L.Garten, and M.Boudart, *J.Catal.* **41**, 40 (1976).

19. R.Rudham and M.K.Sanders, *J.Catal.* **27**, 287 (1972).

20. I.Mochida, S.Hayata, A, and T.Seiyama, *J.Catal.*, **15**, 314 (1969).

21. I.Mochida, T.Jitsumatsu, and T.Seiyama, *Bull.Chem.Soc. Jpn.*, **244**, 2595(1971).

22. C.C.Chao and J.H.Lunsford, *J.Chem.Phys.*, **57**, 2890 (1972).

23. J.Turkevich, Y.Ono, and *J.Catal.*, **25**, 44 (1972).

24. R.G.Herman and D.R.Flentge, *J.Phys., Chem.*, **82**, 720 (1978).

25. Y.Y.Huang, J.Am.Chem.Soc., **95**, 6636 (1973).

26. R.G.Herman , J.H.Lunsford, H.K.Beyer, P.A.Jacobs, and J.B.Uytterhoeven , *J.Phys. Chem.*, **79**, 2388 (1975).

27. Y.Y.Huang and E.F.Vansant, *J.Phys.Chem.* **77**, 663 (1973).

28. S.J.Gentry, N.W.Hurst, and A.Johns, *J.Chem.Soc., Faraday Trans.1*, **75**, 1688 (1979)

29. J.W.Word , *J.Catal.* **11**, 238 (1968).

30. H.Matsumoto, H.Futami, F.Kato, and Y.Morita, *Bull.Chem.Soc.Japan*, **44**, 3170 (1971).

31. M.Sano, T.Maruo, H.Yamatera, M.Suzuki, and Y.Saito, *J.Chem.Soc.*, **109**, 52 (1987).

32. C.M.Naccache and Y.BB.Taarit, *J.Catal.*, **22**, 171 (1971).

33. J.O.Petunchi and W.K.Hall, *J.Catal.*, **80**, 403 (1983).

34. E.E.Miro, D.R.Ardiles, E.A.Lombardo, and J.O.Petunchi, *J.Catal,* **97**, 43 (1986).

35. D.R.Denley, R.H.Raymond, and S.C.Tang, *J.Catal.*, **87**, 414 (1984).

36. P.W.J.G.Wijnen, F.B.M.Van Zon, and D.C.Koningdsberger, *J.Catal.*, **114**, 463 (1988).

37. R.B.Greegor and F.W.Lytle, *J.Catal.*, **63**, 476 (1980).